

# High energy amplitude as an admixture of ‘soft’ and ‘hard’ Pomerons

Sergey Bondarenko <sup>1</sup>, Eugene Levin <sup>1</sup> and C-I Tan <sup>2</sup>

<sup>1</sup> *HEP Department, School of Physics and Astronomy  
Tel Aviv University, Tel Aviv 69978, Israel*

<sup>2</sup> *Physics Department, Brown University,  
Providence RI 02912, USA*

In this paper an attempt is made to find an interface of the perturbative BFKL Pomeron with the non-perturbative Pomeron originating from non-perturbative QCD phenomena such as QCD instantons and/or scale anomaly. The main idea is that the non-perturbative Pomeron involves a large scale ( $M_0 \approx 2 \text{ GeV}$ ), which is larger than the scale from which perturbative QCD is applicable. One key result is that even for processes involving a large hard scale (such as DIS) the low  $x$  behavior is determined by an effective Pomeron with an intercept having an essential non-perturbative QCD contribution.

## I. INTRODUCTION

In this paper we present an attempt to solve one of the most challenging problems of QCD: the interface between long distance (non-perturbative, soft) interaction and the short distance one (perturbative, hard) at high energy. The short distance interaction at high energy is controlled by perturbative QCD and can be described by the BFKL equation [1]. We call the hard Pomeron a solution to this equation, in spite of the fact that this solution is not a Regge pole. The region of long distances we describe by introducing the phenomenological soft Pomeron - a Regge pole with the intercept close to 1 [2]. Recently, progress has been achieved in a theoretical understanding of the structure of the soft Pomeron [3–9], which provides hope for developing a first approach to understand the interface of these two Pomerons: the soft Pomeron and the BFKL one.

This approach is based on a new hierarchy of the scales in QCD suggested in Ref. [3] and depicted in Fig. 1.

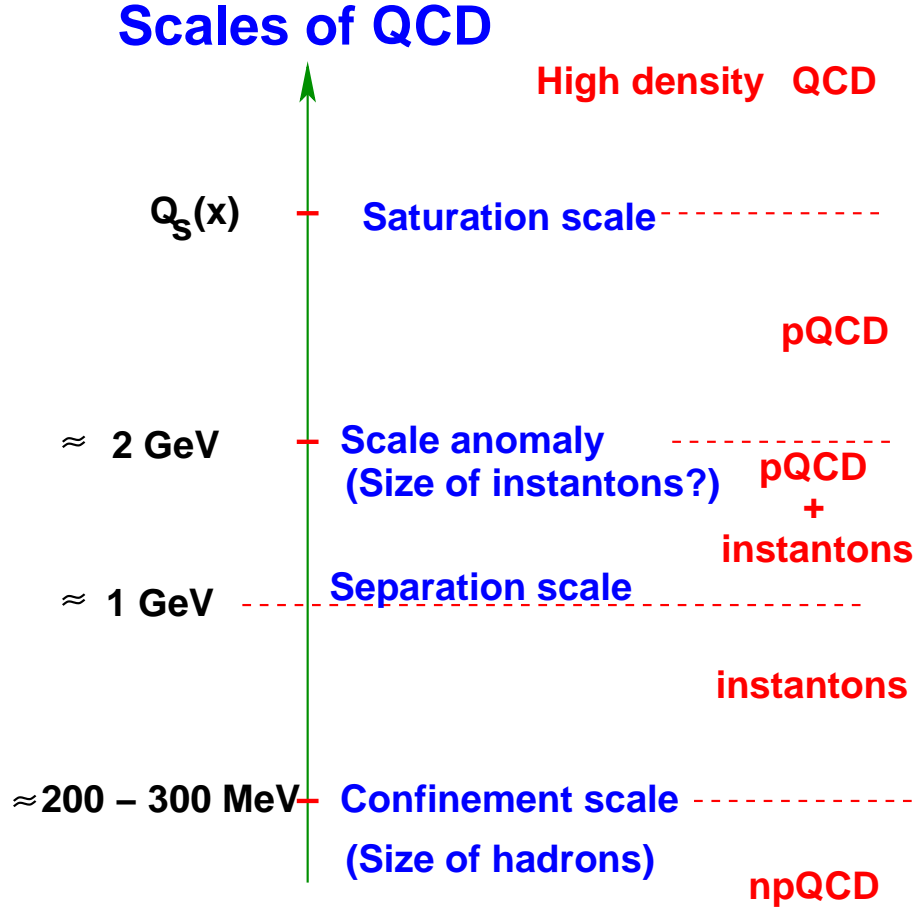


FIG. 1. Scales of QCD accordingly to Ref. [3].

The key idea underlying this picture is the large scale for the soft Pomeron ( $q_S = M_0 \approx 2 \text{ GeV}$ ) which is closely related to the violation of the scale anomaly of QCD. The value of  $M_0$  is so large that the QCD coupling constant  $\alpha_S(M_0) \ll 1$ , and it can be considered to be a small parameter. From Fig. 1 we see that such sequence of scales makes possible a theoretical approach to the problem of interface of soft and hard Pomerons. For all virtualities (transverse momenta) larger than the separation scale,  $q > q_H \approx 1 \text{ GeV}$ , where  $\alpha_S(q^2) < 1$ , we can apply the perturbative QCD approach.

We formulate the problem of the interface between soft and hard Pomeron as a problem of a joint description of the perturbative BFKL Pomeron with the soft Pomeron based on the non-perturbative contributions with sufficiently high scale (see Fig. 1). Many of the non-perturbative contributions originate from very long distances of the order of the confinement scale (see Fig. 1) but we assume that all of them are irrelevant to the structure of the soft Pomeron [3].

We also assume that the energies are so high that the saturation scale [10,11] is much larger than the scale of the anomaly scale, (or the scale of the soft Pomeron),  $q_S \equiv M_0 \approx 2 \text{ GeV}$  and the separation scale  $q_H$  which characterizes that value of the virtuality (transverse momentum) from which we can start using perturbative QCD. Our notation is transparent since  $q_S$  gives the scale of the soft Pomeron, while for  $q > q_H$  we can use the BFKL Pomeron to describe the high energy scattering in pQCD.

In the next section we describe the general formalism of our approach which leads to a new Regge pole as a result of an admixture of soft and hard Pomerons with the trajectory  $\alpha_{S-H}(t) = 1 + \Delta_{S-H} + \alpha'_{S-H} t$ . Section 3 is devoted entirely to the properties of the Green's function of the BFKL Pomeron with the running QCD coupling constant. As it has been shown in many papers [10,12–18] the QCD running coupling constant changes the character of the singularity in the BFKL Pomeron which becomes an essential singularity at  $\omega \rightarrow 0$  instead of a pole at  $\omega = \omega_L$ . In this section we present a detailed analysis of the Green's function

for the BFKL equation which is similar to that of paper [18] which appeared after we had completed our calculations.

In section 4 we calculate the trajectory of the soft Pomeron which leads to the phenomenological Pomeron ( $\alpha_{phenom.P} = 1 + 0.08 + 0.25 \text{ GeV}^{-2} t$  [2]) and which appears as a result of the admixture of the BFKL and soft Pomerons in our approach. The deep inelastic scattering in the region of rather low virtualities of photon is discussed in section 5 where the values of virtualities for the hard processes are specified using our approach for admixture of “soft” and “hard” Pomerons.

## II. GENERAL APPROACH

In this section we outline the general approach for dealing with the interface of soft and hard Pomerons. To do this we need to specify our description of the soft Pomeron based on general ideas of Ref. [3]. We next review the key feature of BFKL Pomeron in the LLA, elaborate its Greens’ function in the Airy model, and finally discuss unifying soft and hard Pomerons.

### A. Soft Pomeron

As a working model for the soft Pomeron we shall adopt the QCD instanton approach [4]. This is in fact not necessary since we only need to use general properties of the soft Pomeron exchange depicted in Fig. 2.

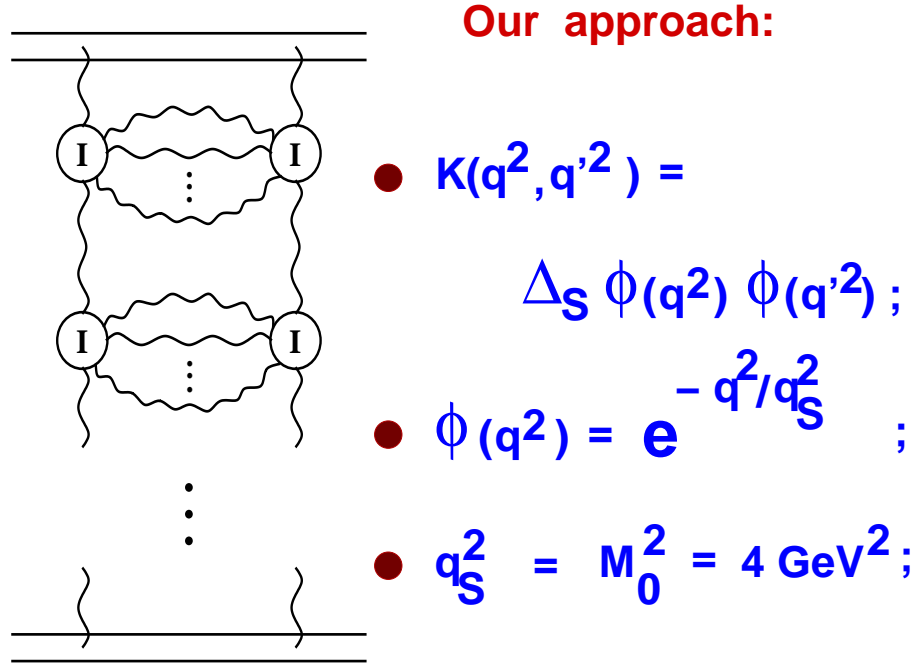


FIG. 2. The main properties of the soft Pomeron originating from the QCD instanton approach [4]

As shown in Ref. [4], the structure of the soft Pomeron in the instanton approach formally reduces to summing the ladder diagrams of Fig. 2. These ladder diagrams describe the  $t$ -channel gluon that propagates through the space inducing a chain of instanton transitions between different vacua and producing a number of gluons in each transition. The sum of these diagrams leads to power-like (Regge-type) asymptotic amplitude, namely the scattering amplitude  $A(s, t)$  is asymptotically equal to

$$A(s, t) = g(t) s^{\alpha_{SP}(t)} , \quad (1)$$

with  $\alpha_{SP}(t) = 1 + \Delta_S + \alpha'_S t$ . It is well known (see Ref. [19]) that both  $\Delta_S$  and  $\alpha'_S$  can be found as solutions of the Bethe-Salpeter type equation resulting from these ladder graphs. In this paper, we shall concentrate on the forward scattering limit,  $t = 0$ , where the kernel  $K(q^2, q'^2)$  is a function of transverse momenta,  $q$  and  $q'$ , along adjacent rungs of the ladder in Fig. 2. We assume that this kernel has the general factorized properties, namely  $K(q^2, q'^2) = \Delta_S \phi(q^2) \phi(q'^2)$  which follow from the instanton approach of Ref. [4] but this could be more general.

### B. BFKL Pomeron

The BFKL Pomeron gives the high energy asymptotic behavior for the scattering amplitude in the so-called leading  $\log(1/x)$  approximation (LLA) of perturbative QCD [1]. In the LLA, for each set of Feynman diagrams of the order of  $\alpha_s^n$ , one keeps only leading terms proportional to  $(\alpha_s \ln(1/x))^n$ , and sum over these terms. In LLA this sum formally reduces to a summation of “gluon ladder” diagrams, (see Fig. 3).

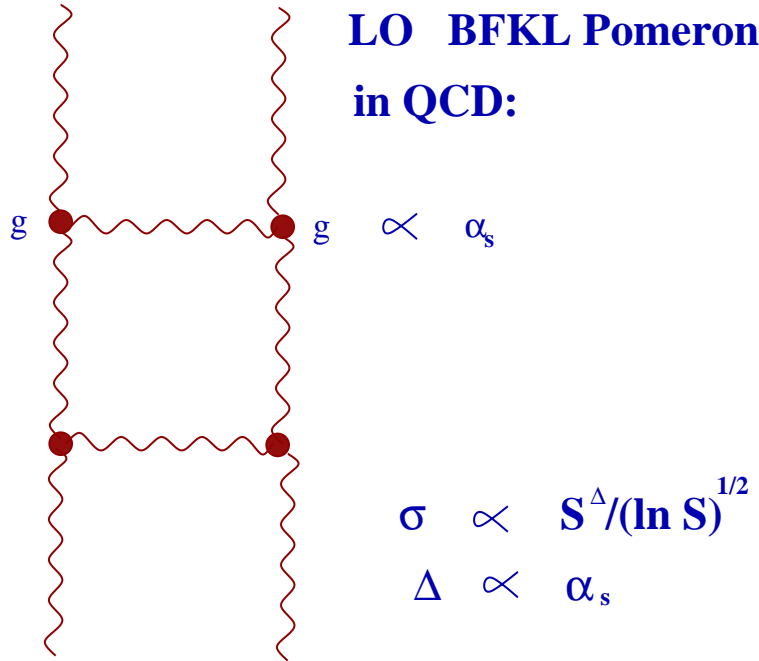


FIG. 3. The BFKL Pomeron in LLA.

However, due to the specific property of the vertex [1], the sum of these “ladder” diagrams leads to an amplitude  $A(s, t) \propto s^{\Delta_H} / \sqrt{\ln(s)}$ , with  $\Delta_H \propto \alpha_s$ . The presence of the additional  $1/\sqrt{\ln(s)}$  factor reflects the fact that the BFKL Pomeron is actually not a Regge pole.

For further discussion, it is more convenient to work in the complex angular momentum plane,  $l \equiv 1 + \omega$ , and to restrict ourselves to the forward limit  $t = 0$ . In particular, we need to find the Green’s function<sup>1</sup>  $G_\omega(\vec{q}_f, \vec{q}_i)$  for the BFKL equation which satisfies the following equation (see Refs. [15,16,18] for details and Fig. 4 for graphical form of the equation)

$$\omega G_\omega(\vec{q}_f, \vec{q}_i) = \delta^{(2)}(\vec{q}_f - \vec{q}_i) + \int d^2 q' K(\vec{q}_f, \vec{q}') G_\omega(\vec{q}', \vec{q}_i). \quad (2)$$

---

<sup>1</sup>We shall also denote this Green’s function as  $G_\omega^H$  to emphasize that it is responsible for the “hard” perturbative QCD contribution.

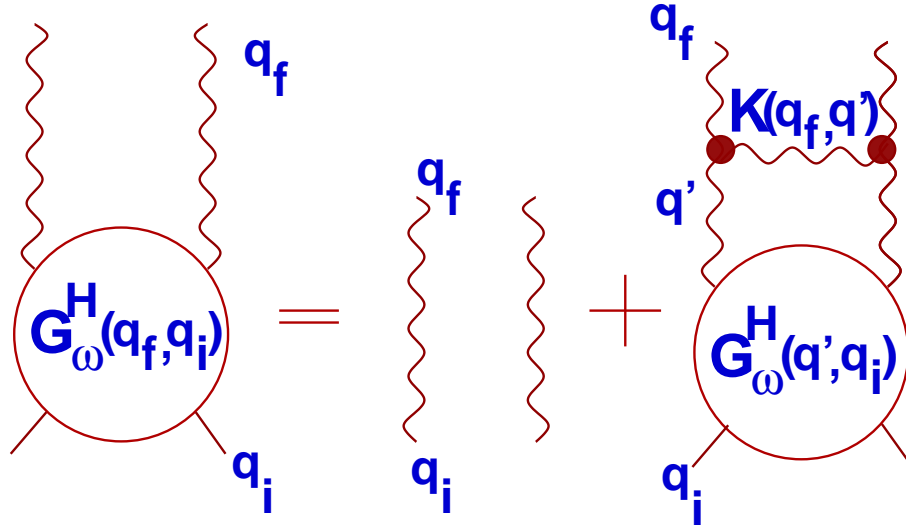


FIG. 4. The BFKL equation for the Green function

The kernel  $K(\vec{q}_f, \vec{q}')$  in Eq. (2) can be written, after integration over the azimuthal angle, in the form

$$K(\vec{q}_f, \vec{q}') = \alpha_s(q_f^2) \tilde{K}\left(\frac{q_f^2}{q'^2}\right). \quad (3)$$

It can be shown that functions

$$\phi_f(q^2) = \left(\frac{q^2}{\sqrt{\alpha_s(q^2)}}\right)^f, \quad (4)$$

satisfy a generalized eigenvalue equation

$$\alpha_s(q^2) \int dq'^2 \tilde{K}\left(\frac{q^2}{q'^2}\right) \phi_f(q'^2) = \frac{r_H}{r} \omega(f) \phi_f(q^2), \quad (5)$$

with  $\omega(f)$  as eigenvalues. Here,  $r = \ln(q^2/\Lambda^2) - \frac{1}{2} \ln \alpha_s(q^2)$ ,  $r_H = \ln(q_H^2/\Lambda^2)$ , and  $\omega(f)$  in leading order of pQCD is equal to

$$\omega(f) = \frac{\alpha_s(r_H) N_c}{\pi} \left\{ 2\psi(1) - \psi\left(\frac{1}{2} - f\right) - \psi\left(\frac{1}{2} + f\right) \right\}. \quad (6)$$

In this paper we will mostly use the expansion of  $\omega(f)$  at small values of  $f$ , namely,

$$\omega(f) = \omega_L (1 + D f^2 + O(f^4)). \quad (7)$$

It should also be stressed that in Eq. (6) and Eq. (7) the normalization point for the QCD running coupling constant  $\alpha_s$  was chosen as the separation scale, namely  $\alpha_s(q_H^2)$ .

The solution to the inhomogeneous Eq. (2) can be found by expanding  $G_\omega(r_f, r_i)$  in terms of the complete set of eigenfunctions, Eq. (4),

$$G_\omega(\vec{q}, \vec{q}_i) \equiv G_\omega(r, r_i) = \int_{a-i\infty}^{a+i\infty} \frac{df}{2\pi i} \chi(\omega, f, r_i) \phi_f(q^2) = \int_{a-i\infty}^{a+i\infty} \frac{df}{2\pi i} \chi(\omega, f, r_i) e^{rf}, \quad (8)$$

$$G(Y; r_f, r_i) = \int \frac{d\omega}{2\pi i} e^{\omega Y} G_\omega(r_f, r_i), \quad (9)$$

where  $Y = \ln(s/q_f q_i)$ .

Using Eq. (8) one obtains the following equation for  $\chi(\omega, f, r_i)$  [16]

$$-\omega \frac{d\chi(\omega, f, r_i)}{df} = r_H \omega(f) \chi(\omega, f, r_i) + r_i e^{-f r_i} . \quad (10)$$

Eq. (10) is a first order differential equation and can be solved analytically. The solution to Eq. (10) can be written as the sum of two terms, [16]:

$$\chi_1(\omega, f, r_i) = \frac{r_i}{2\omega} \int_f^\infty df' e^{-f' r_i + \frac{r_H}{\omega} \int_f^{f'} \omega(f'') df''} , \quad (11)$$

and

$$\chi_2(\omega, f, r_i) = -\frac{r_i}{2\omega} \int_f^{-\infty} df' e^{-f' r_i + \frac{r_H}{\omega} \int_f^{f'} \omega(f'') df''} , \quad (12)$$

where the integration path in Eq. (11) is a ray  $C_1$ , from  $f$  to infinity, lying between the polar angles  $\pi/3$  and  $\pi/2$  and the corresponding path for Eq. (12) is another ray  $C_2$  from  $f$  to minus infinity, lying between the polar angles  $-\pi/3$  and  $-\pi/2$ . For  $G_\omega(r_f, r_i)$ , we obtain

$$G_\omega(r_f, r_i) = \int_{\bar{f}-i\infty}^{\bar{f}+i\infty} \frac{df}{2\pi i} e^{f r_f} (\chi_1(\omega, f, r_i) + \chi_2(\omega, f, r_i)) . \quad (13)$$

It is worthwhile mentioning that the difference between Eq. (11) and Eq. (12) is a solution to the homogeneous BFKL equation with the running QCD coupling constant, (Eq. (10) without the inhomogeneous term). The fact that  $\chi(\omega, f, r_i) = \chi_1(\omega, f, r_i) + \chi_2(\omega, f, r_i)$  corresponds to having chosen the integration constant to Eq. (10) in order to ensure that  $G_\omega(r_f, r_i)$  is real.

### C. The BFKL Green function in the Airy model

To clarify the main properties of the Green's function we consider the expansion of Eq. (7) which is justified at small values of  $f$  and  $f'$ . We call this approach the Airy model, and it was first done in Ref. [18], our functions will be very close to the Airy functions. Using new variables  $f^+ = f' + f$  and  $f^- = f' - f$ , we can reduce Eq. (13) to the form

$$G_\omega(r_f, r_i) = g(\omega, r_f, r_i) = \frac{r_i}{4\omega} \int_{\bar{f}-i\infty}^{\bar{f}+i\infty} \frac{df^+}{2\pi i} \left( \int_{C_1} df^- e^{\Psi(\omega; f^+, f^-; r_f, r_i)} + \int_{C_2} df^- e^{\Psi(\omega; f^+, f^-; r_f, r_i)} \right) \quad (14)$$

$$\Psi(\omega; f^+, f^-; r_f, r_i) = -\frac{r_f + r_i}{2} f^- + \frac{r_f - r_i}{2} f^+ + \frac{\omega_L r_H}{\omega} f^- \left\{ 1 + \frac{D}{3} \left[ \frac{3}{4} (f^+)^2 + \frac{1}{4} (f^-)^2 \right] \right\} ; \quad (15)$$

Integration paths  $C_1$  and  $C_2$  in Eq. (14) are defined in the same way as in previous section, with the initial point shifted to  $f^- = 0$ .

Since the  $f^+$ -integral is Gaussian, we have

$$g(\omega, r_f, r_i) = \sqrt{\frac{r_i^2}{16\pi\omega\omega_L r_H D}} \left( \int_{C_1} + \int_{C_2} \right) \frac{df^-}{\sqrt{f^-}} e^{-f^- \frac{r_f + r_i}{2} \frac{\omega - \tilde{\omega}}{\omega} + (f^-)^3 \frac{D\omega_L r_H}{12\omega} - \frac{1}{f^-} \left( \frac{\delta r}{2} \right)^2 \frac{\omega}{D\omega_L r_H}} , \quad (16)$$

with the  $\tilde{\omega} = \frac{r_H \omega_L}{r_f + r_i}$  and  $\delta r = r_f - r_i$ . We can further change the variable to:  $\nu = \left( \frac{4\omega}{D\omega_L r_H} \right)^{-1/3} f^-$ , and obtain for our Green's function:

$$g(\omega, r_f, r_i) = \sqrt{\frac{r_i^2}{16\pi\omega\omega_L r_H D}} \left( \frac{4\omega}{\omega_L r_H D} \right)^{\frac{1}{6}} \tilde{A}i(\xi; \zeta); \quad (17)$$

$$\tilde{A}i(\xi; \zeta) = \left( \int_{C_1} + \int_{C_2} \right) \frac{d\nu}{\sqrt{\nu}} e^{-\xi\nu + \frac{\nu^3}{3} - \frac{\zeta^2}{\nu}}; \quad (18)$$

$$\xi = \left( \frac{D\omega_L r_H}{4\omega} \right)^{-\frac{1}{3}} \left\{ \frac{r_f + r_i}{2} - \frac{\omega_L r_H}{\omega} \right\}; \quad (19)$$

$$\zeta = \frac{\delta r}{2} \left( \frac{\omega}{2D\omega_L r_H} \right)^{\frac{1}{3}} \text{ with } \delta r = r_f - r_i; \quad (20)$$

Note, that the right dimension of solution of Eq. (2) must be  $g(\omega, r_f, r_i) / (q_f q_i)$ , but this fact is not important for our later consideration, so we will proceed with the dimensionless function Eq. (17). Once  $g(\omega, r_f, r_i)$  is known, the asymptotic behavior of our Green's function  $G(Y; r_f, r_i)$  can be obtained from Eq. (9). However, in dealing with the general expression ( see Eq. (17) - Eq. (20) ) we have to take into account that the limit depends on the virtualities  $r_f$  and  $r_i$  and, in particular, the value  $\tilde{\omega}$ . Further, ultimately, we need also to take into account the soft Pomeron intercept. For different relations between these two values, different region in the  $\omega$  integral can dominate, leading to different asymptotic behavior for the Green's function. We start the search for the resulting singularities by considering various situations where different regions of  $\omega$  dominate the integral in Eq. (9).

We first consider the case when  $\omega \gg \tilde{\omega}$ . In this region both  $\xi$  ( Eq. (19)) and  $\zeta$  (Eq. (20)) are large, and therefore the main contribution in this integral comes from the region of small  $\nu$ . Neglecting the  $\nu^3$  term in the exponent of the integrand, we obtain

$$\tilde{A}i(\xi; \zeta) \propto \int_0^\infty \frac{d\nu}{\sqrt{\nu}} e^{-\nu\xi - \frac{1}{\nu}\zeta^2} \quad (21)$$

We will see later, that omitted  $e^{\nu^3/3}$  term is indeed small. For such an integral the integration over two different contours in Eq. (13) give the same answer, since the integrand has no singularities in the right semi plane and both integrals could be taken along the real axis. The resulting integral can be evaluated explicitly, leading to:

$$\tilde{A}i(r_i, r_f) \propto 2K_{-1/2} \left( 2(\delta r/2) \sqrt{\frac{\omega - \tilde{\omega}}{\tilde{\omega} D}} \right) \left( \frac{\zeta}{\xi^{1/2}} \right)^{1/2} \quad (22)$$

where  $K_\nu(z)$  is the modified (McDonald) Bessel function. Since Eq. (21) does not depend on the sign of  $\delta r$ , we can therefore write the answer as

$$g(\omega, r_f, r_i) = G_\omega^1(r_f, r_i) = \frac{r_i}{2\tilde{r}^{1/2}} \sqrt{\frac{1}{\omega\omega_L r_H D}} \left( e^{-2(\frac{\delta r}{2})\sqrt{\frac{\omega - \tilde{\omega}}{D\tilde{\omega}}}} \theta(\delta r) + e^{2(\frac{\delta r}{2})\sqrt{\frac{\omega - \tilde{\omega}}{D\tilde{\omega}}}} \theta(-\delta r) \right). \quad (23)$$

Instead of integrating over  $\delta r$ , we could simply integrate over the following function for positive values of  $\delta r$ :

$$G_\omega^1(r_f, r_i) = \frac{r_i}{\tilde{r}^{1/2}} \sqrt{\frac{1}{\omega\omega_L r_H D}} e^{-2(\frac{\delta r}{2})\sqrt{\frac{\omega - \tilde{\omega}}{D\tilde{\omega}}}}, \quad (24)$$

where  $\tilde{r} = \frac{r_i + r_f}{2} - \frac{\omega_L r_H}{\omega}$ . In this region,  $\delta r$  and  $\nu$  are small,  $\delta r \sim \sqrt{\frac{D\tilde{\omega}}{\omega - \tilde{\omega}}} \ll 1$  and  $\nu \propto \frac{\zeta}{\xi^{1/2}} \sim \left( \frac{\tilde{\omega}}{32\omega} \right)^{1/3} \ll 1$ . Therefore, we can trust this solution so long that the following condition is satisfied:

$$\frac{\tilde{\omega}}{\omega} \leq 1. \quad (25)$$

Indeed, even when  $\frac{\tilde{\omega}}{\omega} = 1$ , the  $\nu$  is still small,  $\nu \sim \left( \frac{1}{32} \right)^{1/3} \ll 1$ . The magnitude of the omitted term in our solution is also small, namely,  $e^{\frac{1}{96} \frac{D\tilde{\omega}}{\omega(\frac{r_f + r_i}{2})^2}}$ , and we have for the Green's function in this region:

$$G_{\omega}^1(r_f, r_i) = \frac{r_i}{\tilde{r}^{1/2}} \sqrt{\frac{1}{\omega \omega_L r_H D}} e^{-\delta r \sqrt{\frac{\omega - \tilde{\omega}}{D \tilde{\omega}} + \frac{1}{96} \frac{D \tilde{\omega}}{\omega (\frac{r_f + r_i}{2})^2}}}, \quad (26)$$

This equation gives the asymptotic answer for the Green's function for the case  $\omega \gg \tilde{\omega}$ , in the so called diffusion approximation for the BFKL kernel. The Mellin transform of Eq. (26) gives:

$$G^1(Y; r_f, r_i) = \sqrt{\frac{1}{2\pi Y \tilde{\omega} D}} e^{-\frac{(\delta r)^2}{4Y \tilde{\omega} D}} \quad (27)$$

( see calculations in Appendix A ).

There is another contribution in the limit of  $\omega \gg \tilde{\omega}$  coming from the large  $\nu$  region. Indeed, it is easy to see from Eq. (18), that there is another saddle point,

$$\nu_{SP}^2 - \xi \simeq 0. \quad (28)$$

In the region  $\xi \gg 1$  we have

$$\nu_{SP} = \sqrt{\xi} = r_f^{\frac{1}{2}} \frac{\sqrt{\omega - \tilde{\omega}}}{\omega^{\frac{1}{3}}} (\omega_L r_H D/4)^{-\frac{1}{6}} \gg 1. \quad (29)$$

This saddle point corresponds to the second crossing point of Fig. 5. This is a solution for the  $\omega > \tilde{\omega}$ .

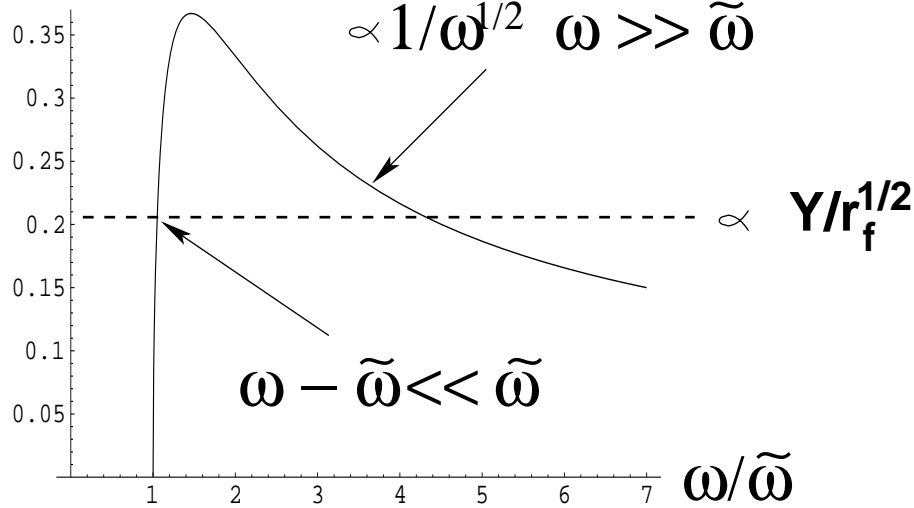


FIG. 5. The positions of the saddle points in  $\omega$  for  $G(y; r_f, f_f)$  for  $\omega > \tilde{\omega}$ .

However, it turns out that in this regime,  $f_{SP}^- \gg 1$  while  $f_{SP}^+$  is small ( $f_{SP}^+ \ll 1$ ). It follows that we can not use the diffusion approach for the BFKL equation to obtain an estimate of this contribution. In this case Eq. (17)-Eq. (18) are no longer valid, and we have to take the full kernel of Eq. (6) into consideration. The integration over this full kernel is performed along the real axis and instead of two solutions Eq. (11) and Eq. (12) now we have one. Going back to the variables  $f^+$  and  $f^-$  and considering  $f^+/f^- \ll 1$ , one can obtain the following equation for the saddle point:

$$r_f - \frac{2r_H}{\omega} \frac{\alpha_s(r_H) N_c}{\pi} \frac{1}{1 - f_{SP}^-} = 0 \quad (30)$$

Eq. (30) stems from the fact that in the region of large  $\omega$ ,  $f^-$  is rather large. For large  $f^-$  we can replace  $\omega(f^-)$  by  $\omega(f^-) \rightarrow \frac{\alpha_s(r_H) N_c}{\pi} \frac{2}{1 - f_{SP}^-}$ . Thus we have

$$1 - f_{SP}^- = \frac{2\tilde{\omega}}{\omega} \ll 1. \quad (31)$$



We obtain for the Green's function in this region of  $\omega$ :

$$G_\omega^2(r_i, r_f) \sim \sqrt{\tilde{\omega}} e^{-\frac{r_i + r_f}{2} - \frac{2\alpha_s(r_H) N_c r_H}{\pi \omega} \ln(\frac{\tilde{\omega}}{\omega})} \quad (32)$$

For the  $\omega$ -saddle point, we have

$$Y + \frac{2\alpha_s(r_H) N_c r_H}{\pi \omega_{SP}^2} \ln(\frac{\tilde{\omega}}{\omega_{SP}}) = 0, \quad (33)$$

which leads to

$$\omega_{SP} = \left( \frac{2\alpha_s(r_H) N_c r_H}{\pi Y} \ln \frac{2\alpha_s(r_H) N_c r_H}{Y \pi \tilde{\omega}^2} \right)^{\frac{1}{2}}. \quad (34)$$

Using Eq. (34), we arrive at

$$G^2(Y; r_f, r_f) \sim e^{2\sqrt{\frac{2\alpha_s(r_H) N_c r_H}{\pi Y} \ln \frac{2\alpha_s(r_H) N_c r_H}{Y \pi \tilde{\omega}^2}}}. \quad (35)$$

This contribution has been missed in Refs. [16,18]. Nevertheless, comparing Green's functions of Eq. (26) and Eq. (32), we see, in the limit of small  $\tilde{\omega}$ , the contribution of Eq. (26) is larger than the contribution of Eq. (32):

$$\frac{G_\omega^2(r_i, r_f)}{G_\omega^1(r_i, r_f)} \sim e^{-\frac{r_i + r_f}{2}}. \quad (36)$$

We next consider the limit where  $\omega$  is close to  $\tilde{\omega}$ :  $\omega = \tilde{\omega} + \delta\omega$ , i.e.,  $\delta\omega/\tilde{\omega} \ll 1$ . In this case  $\xi$  is small,  $\xi \ll 1$ , indeed,  $\xi \sim \frac{\omega - \tilde{\omega}}{\omega} \propto \frac{\delta\omega}{\tilde{\omega}} \ll 1$ , and for small  $\xi$  we have  $\nu \sim 1$ . We also take  $\delta r$  in the limit  $\delta r \ll (r_H D)^{1/3}$  and, therefore, we neglect the  $\zeta^2/\nu$  term in our equation. We now need to consider both solutions of Eq. (10) together, sum of Eq. (11) and Eq. (12). Due to the integration along the rays  $\pi/3$  and  $-\pi/3$  we have :

$$g(\omega, r_f, r_f) \propto e^{i\pi/6} \int_0^\infty \frac{d\nu}{\sqrt{\nu}} e^{-\xi \nu e^{i\pi/3} - \frac{\nu^3}{3}} + e^{-i\pi/6} \int_0^\infty \frac{d\nu}{\sqrt{\nu}} e^{-\xi \nu e^{-i\pi/3} - \frac{\nu^3}{3}} \quad (37)$$

and finally we obtain ( see calculations in Appendix A ):

$$g(\omega, r_f, r_f) \propto \frac{\Gamma(\frac{1}{6})}{3^{2/3}} - \left( \frac{4\omega}{D\omega_L r_H} \right)^{2/3} \frac{(\frac{r_i + r_f}{2})^2}{8\omega^2} (\delta\omega)^2 \frac{\Gamma(\frac{5}{6})}{3^{4/3}}. \quad (38)$$

The Mellin transform of Eq. (38), see Appendix A, gives:

$$G(Y; r_f, r_i) = \sqrt{\frac{3r_i}{8\pi Y \omega_L r_H D}} e^{\tilde{\omega} Y - \frac{2}{9\sqrt{3}} \frac{D(\tilde{\omega} Y)^3}{(r_f + r_i)^{2/4}}}. \quad (39)$$

The region of applicability of this saddle point analysis stems from condition that  $f^+$  and  $f^-$  should be small in order to use the expansion of Eq. (7) and from  $\omega_{SP} < \tilde{\omega}$ . It is easy to see that these conditions restrict the value of rapidity  $Y$  [13–16,18]

$$0 < Y < \frac{r_f^2}{\omega_L r_H}. \quad (40)$$

Now, if we consider together the asymptotic behavior of the Green's function given by Eq. (27) and Eq. (39), we see that in a large range of rapidity, given by Eq. (40), the contribution of Eq. (39) is much larger than contribution Eq. (27). Therefore, the main contribution to the Green's function gives the region of such  $\omega$ , where  $\omega \sim \tilde{\omega}$ .

In the region of small  $\omega < \tilde{\omega}$  where  $\xi$  is negative (see Eq. (19) ), the saddle point of  $\nu$  is equal to

$$\nu_{SP} = \pm i \left( \frac{\omega_L r_H}{D \omega} \right)^{\frac{1}{3}} . \quad (41)$$

Performing calculations for the saddle point we arrive at

$$\omega_{SP} = \pm (1 - i) \sqrt{\frac{2 \omega_L r_H}{D 3 Y}} . \quad (42)$$

The Green's function is [18]

$$G(Y; r_f, r_f) \sim e^2 \sqrt{\frac{\omega_L r_H Y}{3 D}} \cos \sqrt{\frac{\omega_L r_H Y}{3 D}} . \quad (43)$$

It turns out that restrictions  $f_{SP}^+ < 1$  and  $f_{SP}^- < 1$  can be satisfied, but only within numerical accuracy, namely,  $f_{SP}^- < 1/D$ . We will see later that  $D$  is rather large.

#### D. Soft to BFKL Pomeron transition

The main idea of the paper is shown in Fig. 6. Generally speaking the sum of diagrams in Fig. 6 can be found as a solution to the following equation:

$$G_{\omega}^{S-H}(r_f, r_i) = D(\omega; r_f, r_i) + D \bigotimes (K_S + K_H) \bigotimes G_{\omega}^{S-H} . \quad (44)$$

where sign  $\bigotimes$  stands for all needed integrations and  $D(\omega; r_f, r_i)$  denotes the Green's function of two gluon exchange. Using the factorization properties of soft Pomeron kernel we can solve this equation, the derivation of the solution is given in Appendix B, and it reads :

$$G_{\omega}^{S-H}(r_f, r_i) = G_{\omega}^H(r_f, r_i) + \frac{\tilde{G}_{\omega}^H(r_f, r_i)}{1 - \Delta_S \int dr' \int dr'' \phi(r') G_{\omega}^H(r', r'') \phi(r'')} , \quad (45)$$

where

$$\tilde{G}_{\omega}^H(r_f, r_i) = \Delta_S \int dr'' \phi(r'') G_{\omega}^H(r_f, r'') \int dr' \phi(r') G_{\omega}^H(r', r_i) . \quad (46)$$

It is easy to see from Eq. (46), that when  $K_S = 0$ , Eq. (45) describes only the “hard” Pomeron. In the case, where there is no pQCD emission, when  $G^H = D$ , Eq. (45) has a form:

$$G_{\omega}^{S-H}(r_f, r_i) = D(\omega; r_f, r_i) + \Delta_S \frac{\int dr'' \phi(r'') D(\omega; r_f, r_i) \int dr' \phi(r') D(\omega; r_f, r_i)}{1 - \Delta_S \int dr' \int dr'' \phi(r') D(\omega; r_f, r_i) \phi(r'')} . \quad (47)$$

Since  $D(\omega; r_f, r_i) = \delta(r_f - r_i)/\omega$ , Eq. (47) leads to

$$G_{\omega}^{S-H}(r_f, r_i) = \frac{\delta(r_f - r_i)}{\omega} + \frac{1}{\omega} \frac{K_S(r_f, r_i)}{\omega - \Delta_S} , \quad (48)$$

or, in other words, we only have the soft Pomeron in this case.

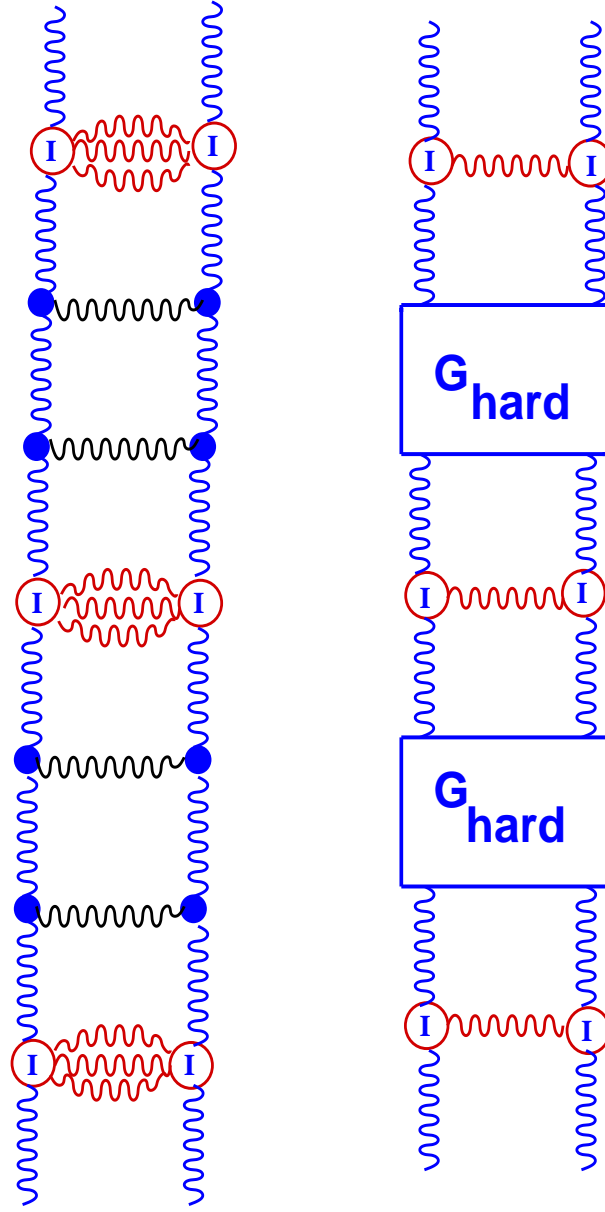


FIG. 6. The diagrams and the graphic form of the equation for soft to BFKL Pomeron transition.

Eq. (45) has poles which are the zeros of the denominator, namely,

$$1 - \Delta_S \int dr' \int dr'' \phi(r') G_\omega^H(r', r'') \phi(r'') = 0. \quad (49)$$

For  $\omega \gg \tilde{\omega}$  the solution of Eq. (49) is (see Appendix C )

$$\omega = \Delta_{S-H} = \Delta_S + \tilde{\omega}_S + \frac{D \tilde{\omega}_S \Delta_S}{96 r_S^2 (\tilde{\omega}_S + \Delta_S)}. \quad (50)$$

Therefore, the intercept of the resulting pole is simply  $\Delta_{S-H} = \Delta_S$  for  $\tilde{\omega}_S \rightarrow 0$ . This result is expected since for  $\tilde{\omega}_S = 0$ , there is no perturbative emission of gluons. It should be stressed, that this answer is obtained with the restriction,

$$\omega \geq \tilde{\omega}_S , \quad (51)$$

see also Eq. (25).

It is easy to see, that this restriction is satisfied when  $\tilde{\omega}_S$  is small. This happens in two cases:

- when  $\bar{\alpha}_S$  is small. In this case  $\tilde{\omega}$  is also small and, therefore, from Eq. (51) we have:

$$\Delta_S \gg \tilde{\omega}_S \sim \tilde{\omega} . \quad (52)$$

We can make a simple numerical estimate: for  $\bar{\alpha}_S \approx 0.1$  we have  $\omega_L \approx 0.18$  ( $\tilde{\omega}_S \approx 0.1$ ) (see next section), so taking  $\omega = \Delta_{S-H} \approx 0.2$  we obtain  $\Delta_S \sim 0.1$ , where  $\Delta_S > \tilde{\omega}_S \sim \tilde{\omega}$ . So, one can see that restriction Eq. (52) is satisfied for  $\bar{\alpha}_S \leq 0.1$ ;

- when  $\tilde{\omega}_S$  is small due to possible large  $r_S$ , namely,

$$r_S \geq \frac{\omega_L r_H}{\Delta_{S-H}} . \quad (53)$$

We next consider another region of  $\omega$ . We assume that the position of the resulting pole  $\omega = \Delta_{S-H}$  may be close to  $\tilde{\omega}_S$ ,  $\Delta_{S-H} = \tilde{\omega}_S + \delta\omega$ , where for  $\delta\omega$  there are two asymptotic limits. The first is the small  $\delta\omega$ ,  $\frac{\delta\omega}{\tilde{\omega}_S} \ll 1$ , and the second for the  $\delta\omega$  of the order of  $\tilde{\omega}_S$ ,  $\frac{\delta\omega}{\tilde{\omega}_S} \sim 1$ . The solution of Eq. (49) in this case is

$$\omega = \Delta_{S-H} = \tilde{\omega}_S + \delta\omega = \frac{2\Delta_S^3 r_S}{\tilde{\omega}_S^2 D^2} \left( \frac{\Gamma(\frac{1}{6})}{3^{2/3}} \right)^3 . \quad (54)$$

Fig. 7 shows the numerical solution to Eq. (54) with  $r_S = r_S^{mat}$  (see later Eq. (58)), and with  $\Delta_S = 0.1$ . We obtain that for  $\Delta_S = 0.1$ ,  $\frac{\delta\omega}{\tilde{\omega}_S} \sim 0.3 - 0.8$ .

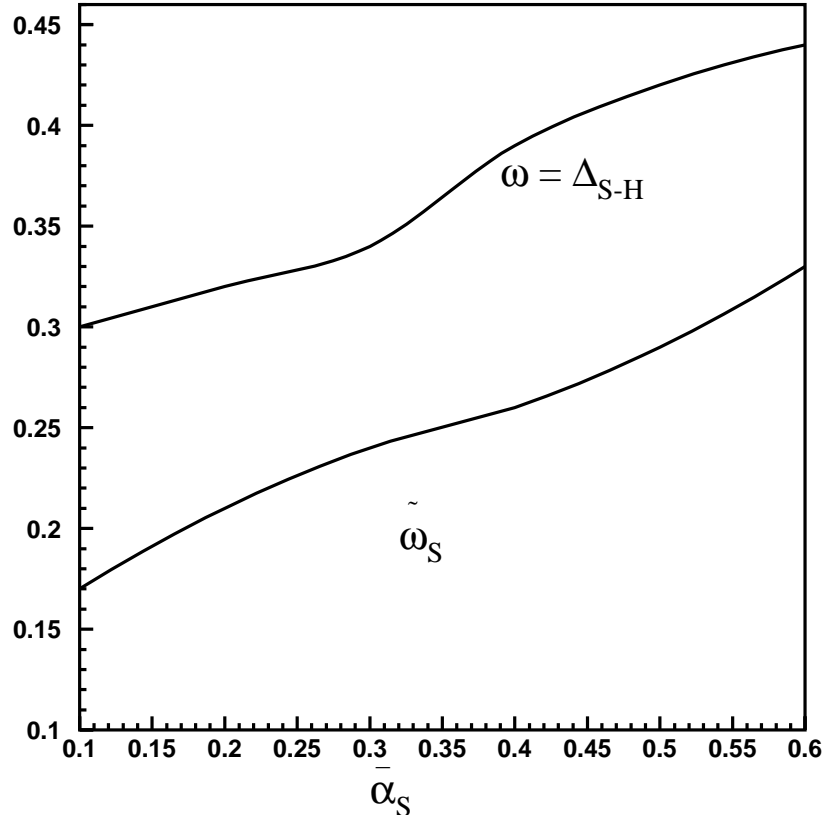


FIG. 7. Solutions for  $\Delta_{S-H}$  and  $\tilde{\omega}_S$  as functions of  $\bar{\alpha}_S$  at  $\Delta_s = 0.1$ .

We can trust this solution only if  $\omega$  is larger than  $\tilde{\omega}_S$ , and this condition can be translated in the following inequality

$$\tilde{\omega}_S < \frac{2\Delta_S^3 r_S}{\tilde{\omega}_S^2 D^2} \left( \frac{\Gamma(\frac{1}{6})}{3^{2/3}} \right)^3. \quad (55)$$

or in the restriction on the value of  $\tilde{\omega}_S$

$$\tilde{\omega}_S \leq \Delta_S \frac{r_S^{1/3}}{D^{2/3}} \frac{2^{1/3} \Gamma(\frac{1}{6})}{3^{2/3}}. \quad (56)$$

Remembering that Eq. (54) is valid only if  $\tilde{\omega}_S \geq \Delta_S$  we see that Eq. (55) is a solution for  $r_S$  which satisfies the inequality

$$\Delta_S \leq \tilde{\omega}_S \leq \Delta_S \frac{r_S^{1/3}}{D^{2/3}} \frac{2^{1/3} \Gamma(\frac{1}{6})}{3^{2/3}}. \quad (57)$$

The solution of Eq. (57) defines the region of  $r_S$  for which we can trust the approximate equation Eq. (54).

In Fig. 8, we present the solution for  $r_S$  to Eq. (57) as a function of  $\bar{\alpha}_S$  at fixed  $\Delta_S = 0.1$ . In Fig. 9, the same solution is plotted versus  $\frac{\omega}{\Delta_S}$  for  $D = 3$ .

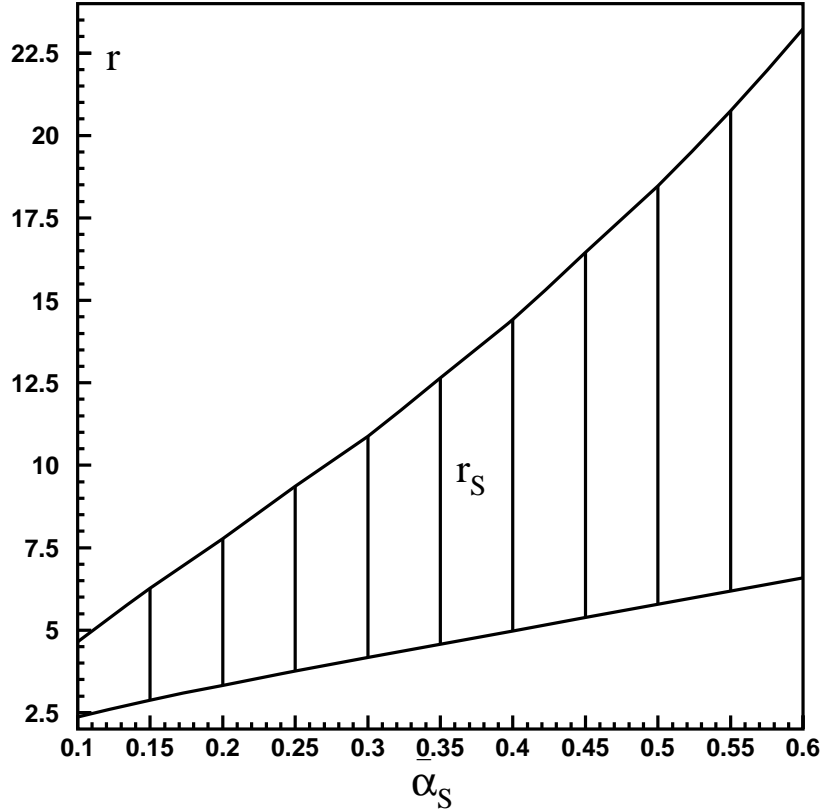


FIG. 8. Permitted  $r_S$  as function of  $\bar{\alpha}_S$  at  $\Delta_S = 0.1$ .

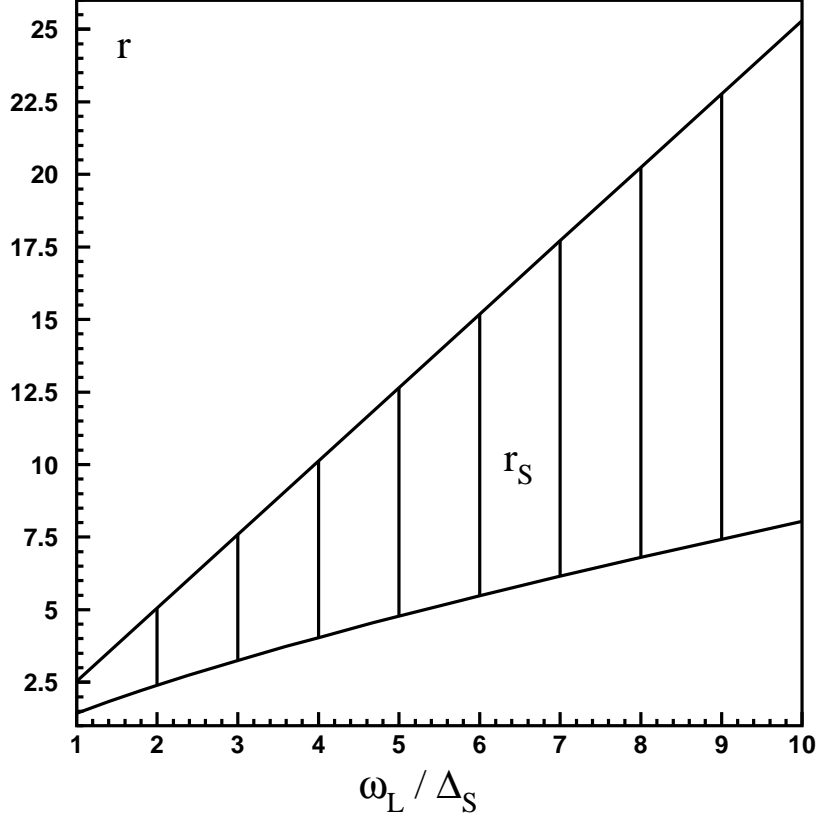


FIG. 9. Permitted  $r_S$  as function of  $\frac{\omega_L}{\Delta_S}$  at  $D = 3$ .

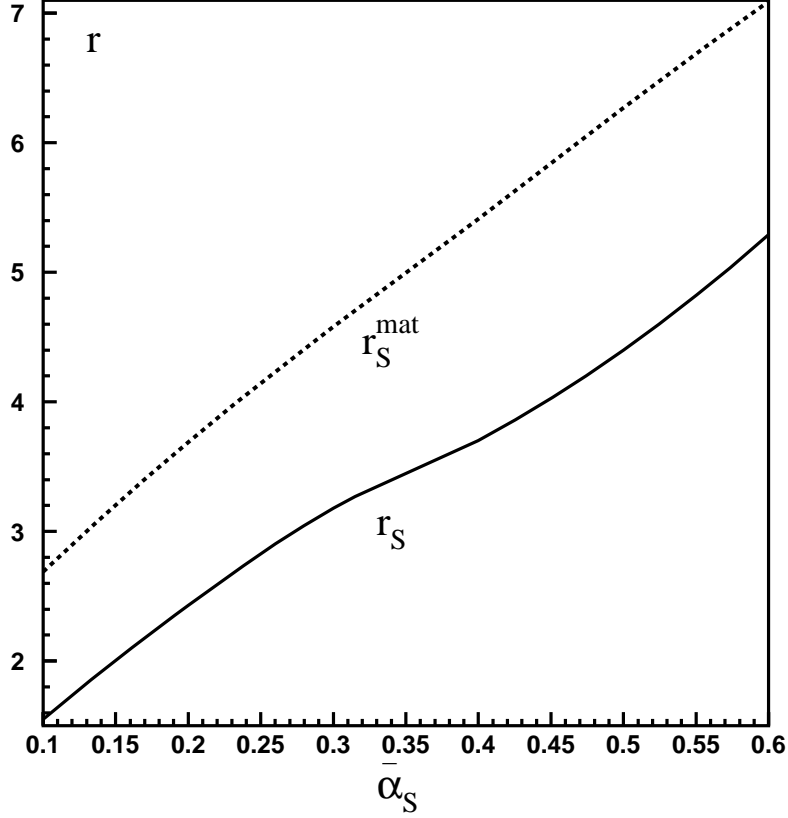
The matching between Eq. (54) and Eq. (50) occurs at  $r_S = r_S^{mat}$ , for which we have

$$\Delta_{S-H} = \Delta_S + \tilde{\omega}_S + \frac{D \tilde{\omega}_S \Delta_S}{96 r_S^2 (\tilde{\omega}_S + \Delta_S)} = \frac{2 \Delta_S^3 r_S}{\tilde{\omega}_S^2 D^2} \left( \frac{\Gamma(\frac{1}{6})}{3^{2/3}} \right)^3. \quad (58)$$

A numerical solution of this equation is presented in Fig. 10. This solution is the function of  $\bar{\alpha}_S$  with  $\Delta_S = 0.1$ . To justify this procedure, we have to show that, for  $r_S = r_S^{mat}$  both solutions, Eq. (54) and Eq. (50), are valid. It is easy to see from Fig. 8 that  $r_S^{mat}$  calculated from Eq. (58) for any value of  $\bar{\alpha}_S$ , is in region where Eq. (54) has solution. From Fig. 7 we also obtain, that for given  $r_S$  the ratio  $\frac{\delta\omega}{\tilde{\omega}_S}$  is  $\frac{\delta\omega}{\tilde{\omega}_S} \sim 0.3 - 0.8$ , and these values satisfy the condition of Eq. (A14), which defines the applicability of this solution. The solution Eq. (54) is valid for  $r_S = r_S^{mat}$ . We next consider the solution given by Eq. (50). The region of applicability of this solution is defined by Eq. (53):

$$r_S \geq \frac{\omega_L r_H}{2 \Delta_{S-H}} \quad (59)$$

The boundary value of  $r_S$ , which is  $r_S = \frac{\omega_L r_H}{2 \Delta_{S-H}}$ , is also presented in the Fig. 10. Considering this picture, we see, that this line lies under the  $r_S^{mat}$  defined by Eq. (58). Remembering, that the ratio  $\frac{\delta\omega}{\tilde{\omega}_S} \sim 0.3 - 0.8$  satisfies the Eq. (25), we obtain, that solution Eq. (50) is also valid for the given values of  $r_S^{mat}$ .



Matching value  $r_S^{mat}$  and boundary value  $r_S$  as function of  $\bar{\alpha}_S$  at  $\Delta_S = 0.1$ .

FIG. 10.

So, finally, we have two solutions, the first is Eq. (50) which is useful for  $r_S$  that lies between the lines of Fig. 10, and second is Eq. (54), which we use when  $r_S$  lies between the line for  $r_S^{mat}$  from Fig. 10 and upper bound of Fig. 8. In the following we will denote all these solutions by the  $\Delta_{S-H}$ .

### III. NLO BFKL

As have been discussed the position of the resulting singularity (pole) crucially depends on the value of  $\tilde{\omega}$  or  $\omega_L$ . In this section we discuss the values of  $\omega_L$  and  $D$  in the NLO BFKL equation [20,21]:

$$\omega = \omega_L (1 + D f^2). \quad (60)$$

NLO BFKL equation leads to the following values of  $\omega_L$  and  $D$  (see Refs. [16,21,22]):

$$\omega_L = \bar{\alpha}_S (q_0^2) (2.772 - 18.3 \bar{\alpha}_S),$$

and

$$D = \bar{\alpha}_S (q_0^2) (16.828 - 322 \bar{\alpha}_S), \quad (61)$$

These values have a serious pathology, as for  $\bar{\alpha}_S > 0.152, (q_0^2 < 30 \text{ GeV}^2)$ ,  $\omega_L$  becomes negative and for  $\bar{\alpha}_S \sim 0.05, (q_0^2 < 3 \times 10^6 \text{ GeV}^2)$   $D$  also changes sign. A solution to this problem was proposed by

G.P.Salam [23] and M.Ciafaloni, D.Colferai and G.P.Salam [17]. They suggested a scheme to improve (resummation) the NLO BFKL kernel. Their resummation is based on the idea that the resummed NLO BFKL kernel should reproduce the NLO DGLAP kernel in the region of large photon virtualities. Indeed, when we start to consider the NLO terms

$$\alpha_s \left( \alpha_s \ln \frac{s}{s_0} \right)^n \quad (62)$$

and change the energy scale in the DGLAP evolution equation, namely,  $s_0 = k_1^2$  ( $k_1^2 \gg k_2^2$ ) to the energy scale  $s_0 = k_1 k_2$  typical for the BFKL approach, the double logarithmic terms arise:

$$\left( \alpha_s \ln^2 \frac{k_1^2}{k_2^2} \right)^{n-m} \left( \alpha_s \ln \frac{k_1^2}{k_2^2} \ln \frac{s}{k_1 k_2} \right)^m. \quad (63)$$

These terms, formally subleading, nevertheless may give significant corrections to the NLO kernel. It was shown [23,17] that these terms are responsible for the difficulties with the NLO kernel. Therefore, the proposed resummation of these double logarithmic terms was done so, that the resummed kernel reproduces a correct DGLAP limit for  $\omega \pm 1/2$  and for a scale  $s_0 = k_1^2$ . Using this method of resummation we can avoid the difficulties of the NLO BFKL kernel. This improved kernel, reproduces correctly the exact NLO BFKL kernel in the region of its applicability, but it turns out to be free from inconsistency of "pure" NLO BFKL kernel. From the proposed different schemes for the improved kernel, see [23], we use scheme number four, as this scheme and also scheme number three has a reasonable behavior of second derivative of the kernel as a function of  $\bar{\alpha}_s$ . As the additional resummation of the terms which are important for the second derivative of the kernel was made.

So we have:

$$\begin{aligned} \bar{\chi}(\gamma \omega \bar{\alpha}_s) = & \bar{\alpha}_s \left( \chi_0(\gamma) - \frac{1}{1/2 - \gamma/2} - \frac{1}{1/2 + \gamma/2} + \frac{1}{1/2 - \gamma/2 + \omega/2 + \bar{\alpha}_s B} + \frac{1}{1/2 + \gamma/2 + \omega/2 + \bar{\alpha}_s B} \right) + \\ & \bar{\alpha}_s^2 \left( \chi_1(\gamma) + \left( B + \frac{1}{2} \chi_0(\gamma) \right) \left( \frac{1}{(1/2 - \gamma/2)^2} + \frac{1}{(1/2 + \gamma/2)^2} \right) \right) + \\ & \bar{\alpha}_s^2 \left( A' \left( \frac{1}{1/2 - \gamma/2} + \frac{1}{1/2 + \gamma/2} - \frac{1}{1/2 - \gamma/2 + \omega/2 + \bar{\alpha}_s B} - \frac{1}{1/2 + \gamma/2 + \omega/2 + \bar{\alpha}_s B} \right) \right). \end{aligned} \quad (64)$$

Here

$$\chi(\gamma, \omega, \bar{\alpha}_s) = \bar{\alpha}_s \chi_0(\gamma) + \bar{\alpha}_s^2 \chi_1(\gamma)$$

is usual BFKL kernel in the next-to-leading order, and

$$B = \frac{11}{8} - \frac{n_f}{12 N_c} + \frac{n_f}{6 N_c^3}, \quad (65)$$

$$A' = -\frac{1}{2} + \frac{5 n_f}{18 N_c} + \frac{13 n_f}{36 N_c^3}. \quad (66)$$

Solving the NLO BFKL equation with improved kernel

$$\omega = \bar{\chi}(\gamma, \omega, \bar{\alpha}_s), \quad (67)$$

we can calculate our NLO  $\omega_L$  and  $D$ . The results are presented in Fig. 11 and Fig. 12, where we also plotted LO  $\omega_L$  and  $D$ . These figures show that the resummed NLO BFKL kernel gives smaller values both for  $\omega_L$  and for  $D$ . From Fig. 11 we obtain  $\tilde{\omega} \approx 0.2$ , which is too high to describe the experimental data for soft processes. On the other hand, namely, this value of the Pomeron intercept describes the inclusive data [29].



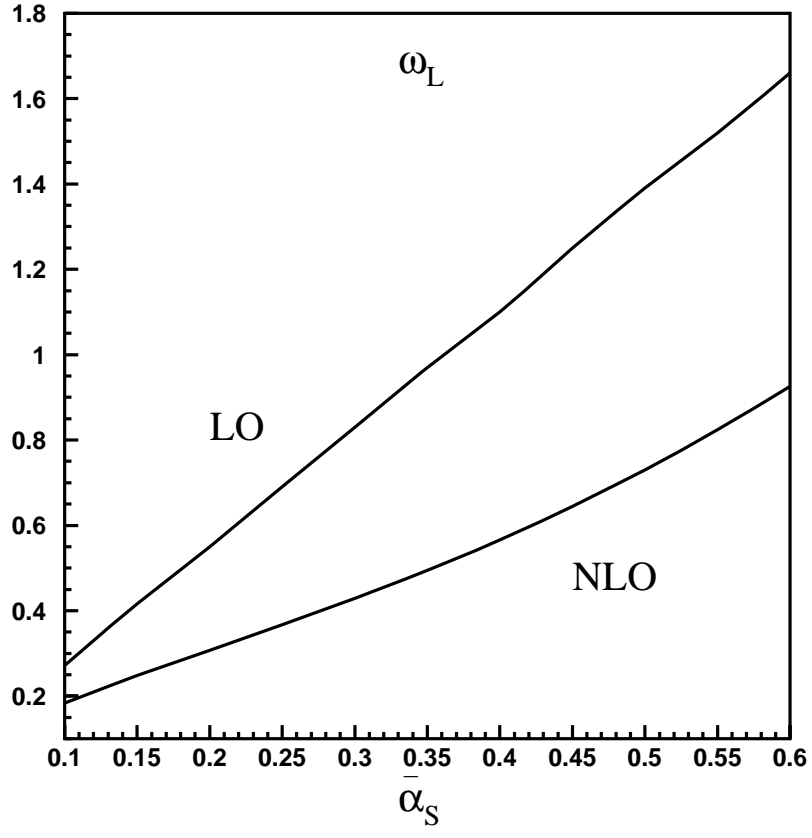


FIG. 11.

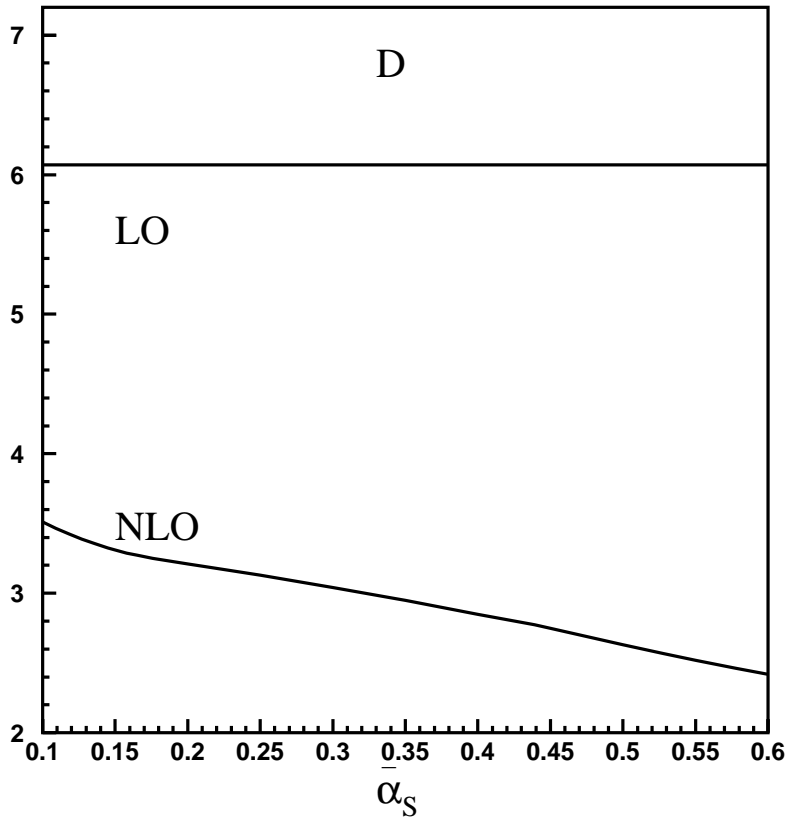


FIG. 12.

#### IV. HARD AND SOFT POMERONS INTERFACE IN DIS

In this section we consider the deep inelastic processes in which we can observe our “effective” Pomeron considering the  $Q^2$  - dependence of the cross section (  $Q^2$  is the photon virtuality) . The diagrams that contribute to DIS are shown in Fig. 13.

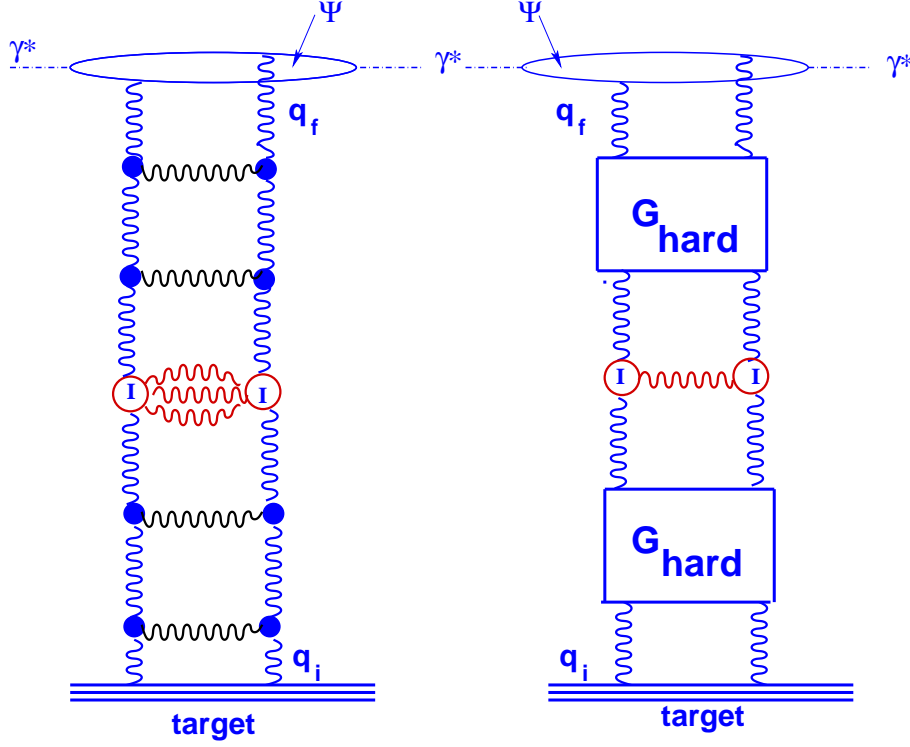


FIG. 13. Diagrams and graphic form of contributions to deep inelastic processes.

The DIS total cross section can be written in the form

$$\sigma_{tot}(\gamma^* p) = \int dr_f dr_i J^{\gamma^*}(Q^2; r_f) G^{DIS}(Y, r_f, r_i) J^N(r_H, r_i), \quad (68)$$

where  $J^{\gamma^*}$  and  $J^N$  are photon and nucleon impact factors, which can be easily calculated in the LO of perturbative QCD (see Refs. [24] and references therein). For example,

$$J^{\gamma^*}(Q^2; r_f) = \int d^2 r_\perp \int_0^1 dz |\Psi(Q^2; r_\perp, z)|^2 (1 - e^{i\vec{q}_f \cdot \vec{r}_\perp}). \quad (69)$$

We introduce the Mellin transform of  $G^{DIS}(Y, r_f, r_i)$  with respect to  $Y$

$$G^{DIS}(Y, r_f, r_i) = \frac{1}{q_f q_i} \int_{a-i\infty}^{a+i\infty} \frac{d\omega}{2\pi i} \left( \frac{s}{q_f q_i} \right)^\omega G_\omega^{DIS}(r_f, r_i). \quad (70)$$

$G_\omega^{DIS}$  is sum of diagrams of Fig. 13 and, therefore, it is equal to  $G_\omega^{S-H}$  given by Eq. (45):

$$G_\omega^{DIS}(r_f, r_i) = G_\omega^H(r_f, r_i) + \Delta_S \frac{\int dr'' \phi(r'') G_\omega^H(r_f, r'') \int dr' \phi(r') G_\omega^H(r', r_i)}{1 - \Delta_S \int dr'' \int dr' \phi(r') G_\omega^H(r', r'') \phi(r'')}. \quad (71)$$

The Green's function of Eq. (71) has a quite different asymptotic behavior than  $g(\omega, r_f, r_i)$  due to the contribution of the denominator. The zero of denominator generates a Regge pole (resulting Pomeron) in  $\omega$ . Therefore, the asymptotic behavior of Green's function of the Eq. (71) depends on what is dominant in given kinematic region, either  $G_\omega^H$  or this pole.

First, we consider the region of rapidity, given by Eq. (40). Now, we have two conditions on  $\Delta_{S-H}$ , which should be satisfied, so that the soft-hard pole contribution in Eq. (71) will dominate. First is the condition of the existence of soft pole solution in denominator of Eq. (71). This condition is given by Eq. (52)-

Eq. (57). Second, we need to check that this soft-hard contribution to the Green's function will give a larger contribution than either the contribution of  $G_\omega^H(r_f, r_i)$  or of the numerator of the second term of Eq. (71). From the derivation of the Eq. (A15)-Eq. (39) is clear, that the asymptotic behavior of both functions in the leading order is given by  $e^{\tilde{\omega} Y}$ . So, all these conditions together define the following restriction for the kinematic region for resulting Pomeron :

$$\Delta_{S-H} \geq \tilde{\omega}. \quad (72)$$

We have obtained this restriction before, see Eq. (52)-Eq. (53), and can say again, that this restriction is satisfied for the case of very small  $\bar{\alpha}_S$ , when  $\bar{\alpha}_S < 0.1$  and therefore  $\Delta_S > \tilde{\omega}_S \sim \tilde{\omega}$ , or for the case of large  $\frac{r_i + r_f}{2}$ , when  $\frac{r_f + r_i}{2} > \frac{\omega_L r_H}{\Delta_{S-H}}$ . So, in both these cases asymptotic behavior of Green's function will be defined by resulting pole. Otherwise, we have the answer of Eq. (39):

$$G(Y; r_f, r_i) = \sqrt{\frac{3 r_i}{8 \pi Y \omega_L r_H D}} e^{\tilde{\omega} Y - \frac{2}{9 \sqrt{3}} \frac{D (\tilde{\omega} Y)^3}{(r_f + r_i)^{2/4}}} \quad (73)$$

in the region of rapidity:

$$0 < Y < \frac{r_f^2}{\omega_L r_H}. \quad (74)$$

Another possibility for the resulting Pomeron dominance is to have large values of rapidity. In this case the Eq. (73) is not valid anymore, and we have to use equations Eq. (41)-Eq. (43). So, using Eq. 42, we can claim that for:

$$\Delta_{S-H} \geq \omega_{SP} \quad (75)$$

we obtain the constraint on the value of rapidity for which the resulting Pomeron governs the high energy asymptotic:

$$Y \geq \frac{\omega_L r_H}{D \Delta_S^2} \quad (76)$$

Let's assume now, that we have resulting Pomeron regime, i.e. consider only the second term of Eq. (71). We want to rewrite our Green's function and estimate the resulting Pomeron contribution. For that, first of all, we have to expand the denominator of resulting Pomeron, Eq. 71, with respect to  $(\omega - \Delta_{S-H})$  :

$$1 - \Delta_S \int dr' \int dr'' \phi(r') G_\omega^H(r', r'') \phi(r'') \approx 1 - \frac{\Delta_S}{\omega - \tilde{\omega}_S} \approx 1 - \left( \frac{\Delta_S}{\omega - \tilde{\omega}_S} \right)_{\omega=\Delta_{S-H}} - \Delta_S (\omega - \Delta_{S-H}) \frac{\partial}{\partial \omega} \left( \frac{1}{\omega - \tilde{\omega}_S} \right)_{\omega=\Delta_{S-H}} + \dots \approx \frac{(\omega - \Delta_{S-H})}{\Delta_S}.$$

Here we take  $\delta\omega$  and  $\Delta_{S-H}$  from Eq. (50). Using this expansion, we rewrite our Green's function:

$$G^{DIS}(Y, r_f, r_i) = \frac{\Delta_S}{q_f q_i} \int_{a-i\infty}^{a+i\infty} \frac{d\omega}{2\pi i} \left( \frac{s}{q_f q_i} \right)^\omega \frac{\tilde{g}(\omega, r_f, r_i)}{\omega - \Delta_{S-H}}, \quad (77)$$

where

$$\tilde{g}(\omega, r_f, r_i) = \int dr'' \phi(r'') G_\omega^H(r_f, r'') \int dr' \phi(r') G_\omega^H(r', r_i)$$

Taking the contour integration we obtain the answer:

$$G^{DIS}(Y, r_f, r_i) = \frac{\Delta_S}{q_f q_i} \left( \frac{s}{q_f q_i} \right)^{\Delta_{S-H}} \tilde{g}(\omega = \Delta_{S-H}, r_f, r_i), \quad (78)$$

or using the Green's function of Eq. (C3) we have:

$$G^{DIS}(Y; r_i, r_f) \approx \frac{\Delta_S r_S^2}{q_f q_i} \frac{\Delta_{S-H}^{-2/3}}{(\omega_L r_H D)^{4/3}} \left( \frac{s}{q_f q_i} \right)^{\Delta_{S-H}}. \quad (79)$$

So, from this consideration, we see, that we have the resulting, phenomenological, Pomeron contribution, determined by Eq. (79), in the following cases:

- first, in the range of rapidity

$$0 < Y < \frac{r_f^2}{\omega_L r_H},$$

for the small values of  $\bar{\alpha}_S$ :  $\bar{\alpha}_S < 0.1$ ;

- second, in the range of rapidity

$$0 < Y < \frac{r_f^2}{\omega_L r_H},$$

for the large values of  $\frac{r_i + r_f}{2}$ :

$$\frac{r_f + r_i}{2} > \frac{\omega_L r_H}{\Delta_{S-H}} \sim r_S;$$

- third, for large rapidities:

$$Y \geq \frac{\omega_L r_H}{D \Delta_S^2}.$$

One can see from Eq. (77) that the soft-hard transition generates a Pomeron satisfying the initial condition for the moments of the deep inelastic structure function. Therefore, in the kinematic region, where the  $\Delta_{S-H}$  contributes, the DGLAP evolution equations only affect the  $Q^2$  dependence of the deep inelastic structure function, while the energy dependence is entirely determined by the soft Pomeron. Such a situation has been studied in details in Ref. [26]. In other kinematic regions we have a normal DGLAP evolution equation with the initial conditions which do not contain the soft-hard Pomeron contributions.

It should also be stressed that at fixed virtuality  $Q^2$  at high energy, asymptotic behavior is determined by the exchange of the soft Pomeron independent of the value of  $Q^2$ . However, the coupling of the soft-hard Pomeron to the photon depends on the value of the photon virtuality.

Estimating our function, Eq. (79), for the case of large  $Q^2$ , we see that the contribution of the rightmost singularity (soft-hard Pomeron) is small at large  $q_f$ . This fact makes our life more complicated and we have to remember the infinite number of the poles that we have in Eq. (45). Indeed, these poles accumulate to zero, as will be seen latter, and, therefore, we face the problem of an essential singularity at zero, which possibly may give a large contribution to the Green's function. We have to estimate the contribution of these secondary poles in  $G^{DIS}(Y; r_i, r_f)$ . This estimate is considered in Appendix D, and the answer is

$$G^{DIS}(Y; r_f, r_i) = \frac{r_i 2^{-1/3}}{\Delta_S \sqrt{\pi} D^{5/6}} \sum_n (-1)^n \frac{((\tilde{A}i(\xi; \zeta))_{r_i=r_S} (\tilde{A}i(\xi; \zeta))_{r_f=r_S})_{\omega=\omega_n}}{(\pi n)^{4/3}} e^{\frac{2}{3} (\frac{4}{D})^{\frac{1}{2}} \frac{r_H \omega_L}{\pi n} \ln \frac{s}{q_i q_f}}. \quad (80)$$

The estimate of the value of this sum we may perform using the method of steepest descent. This estimate gives the  $e^{\sqrt{\ln(s)}}$  behavior for the sum, and this contribution is smaller, than the contribution from the rightmost singularity,  $\Delta_{S-H}$ . Therefore, in our calculation, we can only need consider the resulting Regge pole contribution and neglect the contribution of the secondary poles.

## V. CONCLUSION

This paper is a realization of old ideas to interface non-perturbative Pomeron and perturbative BFKL Pomeron [28]. The new ingredient in our approach is that the typical scale for the “soft” Pomeron is considered [3,4] to be rather large ( $M_0 \approx 2 \text{ GeV}$  or  $r_S = \ln(M_0^2/\Lambda^2) \approx 4.6$ ), larger than the values of transverse momenta ( $p_t$  for which we can use perturbative BFKL approach ( $p_t \geq 1 \text{ GeV}$ ,  $r_H \approx \ln(1 \text{ GeV}^2/\Lambda^2) = 3.2$ ). In other words, we assume that  $r_S \geq r_H$ .

We hoped that taking into account the running QCD coupling constant we would obtain the resulting singularity which would govern “soft” processes close to unity, as it appears in the experimental observations [2]. This hope is based on the fact that the BFKL Pomeron with running QCD coupling leads to a singularity at an angular momentum which is equal to unity. However, it turns out that even for running  $\alpha_s$  the resulting singularity is located to the right of  $\omega_S = \omega_{BFKL}^{r_H}$ . Using the next-to-leading order BFKL estimates for  $\omega_{BFKL} \approx 0.2$  [20,21,23], we obtain  $\omega_S = 0.139$  which is larger than the Pomeron intercept of the D-L phenomenological Pomeron [2]. The estimate of the Pomeron intercept from the single inclusive production suggests a higher value of the Pomeron intercept [29] which is in better agreement with our prediction.

The main result of this paper is concentrated in Eq. (50) and Eq. (54) which give the position of the resulting singularity for different ranges of  $\alpha_s$  and non-perturbative input  $\Delta_S$ . We also discussed the interplay between the BFKL Pomeron and the resulting Pomeron in deep inelastic processes which provide a possibility to measure the hard BFKL Pomeron at large virtualities of photon, and to investigate the interface between the “soft” and the “hard” Pomerons for small values of the photon virtualities. To our surprise our result shows (see Eq. (79)) that even at large photon virtualities the contribution of the resulting singularity dominates at high energy (low  $x$ ). In other words we cannot consider DIS at low  $x$  as a typical hard process where we can safely use perturbative QCD. The admixture of non-perturbative interaction is so essential that it changes the effective Pomeron intercept.

It is interesting to compare our model with the model introduced in Ref. [18], where two Pomeron model was also introduced. We have no ideological disagreements with this model but we differ from it in the way a transition from soft to hard Pomerons occurs and in the origin of soft Pomeron. We assumed that the existence of the soft Pomeron is related to typical non-perturbative phenomena e.g. QCD instantons and/or the scale anomaly in QCD, while in Ref. [18] M. Ciafaloni, M. Taiuti and A. H. Mueller study a possibility that the non-perturbative Pomeron would be generated by the behavior of the QCD coupling at low values of transverse momenta. Our “soft” Pomeron has normal Gribov diffusion in impact parameter space which we admixture with diffusion in transverse momenta typical for the BFKL Pomeron. The freezing of the QCD coupling leads to a new picture which was suggested in Ref. [27] and which is certainly an alternative approach to ours.

We would like to stress that in this paper we consider only the interface of two Pomerons: the soft Pomeron and the BFKL Pomeron. The reality could be much richer and could possibly lead to another scenario of interface the long distance interaction with the short distance QCD physics. As was pointed out in Ref. [30], the soft Pomeron could be suppressed if it is built from QCD instantons, [4], in the high parton density environment. In other words, if the interface between long and short distances interaction passes the stage of high parton density QCD, the soft Pomeron does not contribute to the high energy asymptotic behavior of the scattering amplitude.

The main result of this paper we consider to be the observation that the non-perturbative correction could be essential for so called “hard” process at low  $x$  and large scale of hardness (like DIS at low  $x$ ).

### Acknowledgments:

We wish to thank Jochen Bartels, Errol Gotsman and Uri Maor for very fruitful discussions on the subject. We are very grateful to our referee for all his remarks which, we hope, improves our presentation.

We would like to thank the DESY Theory Group and the BNL Nuclear Theory Group for their hospitality and creative atmosphere during several stages of this work.

E.L. is indebted to the Alexander-von-Humboldt Foundation for the award that gave him a possibility to work on high energy physics during the last year.

This research was supported in part by the GIF grant # I-620-22.14/1999, and by the Israel Science Foundation, founded by the Israeli Academy of Science and Humanities.

Special thanks go to the Dima Kharzeev and Yuri V. Kovchegov who took part in the first part of the research and whose discussions and support were very helpful.

## APPENDIX A

We consider the mellin transform over  $\omega$  in Eq. (26) with the contour of integration defined in a usual way: to the right of all singularities of the integrand. First consider the limit  $Y \rightarrow 0$ :

$$G^1(0; r_f, r_i) = \frac{2r_i}{r_i + r_f} \sqrt{\frac{1}{\tilde{\omega} D}} \int_{\tilde{\omega} - i\infty}^{\tilde{\omega} + i\infty} \frac{d\omega}{2\pi i} \frac{e^{-\delta r \sqrt{\frac{\omega - \tilde{\omega}}{D \tilde{\omega}}}}}{\sqrt{\omega - \tilde{\omega}}}. \quad (\text{A1})$$

Closing the contour of integration to the left over the cut from the  $-\infty$  to  $\tilde{\omega}$  with the variables change:

$$\omega - \tilde{\omega} = e^{i\pi} \delta\omega \quad (\text{A2})$$

on the upper edge of the cut, and

$$\omega - \tilde{\omega} = e^{-i\pi} \delta\omega \quad (\text{A3})$$

on the lower edge of the cut. In so doing, the integral Eq. (A1) turns into a sum:

$$G^1(0; r_f, r_i) = -\frac{2r_i}{r_i + r_f} \sqrt{\frac{1}{\tilde{\omega} D}} \int_0^\infty \frac{d\delta\omega}{2\pi i} \frac{e^{-i\delta r \sqrt{\frac{\delta\omega}{D \tilde{\omega}}}}}{i\sqrt{\delta\omega}} - \frac{2r_i}{r_i + r_f} \sqrt{\frac{1}{\tilde{\omega} D}} \int_\infty^0 \frac{d\delta\omega}{2\pi i} \frac{e^{i\delta r \sqrt{\frac{\delta\omega}{D \tilde{\omega}}}}}{-i\sqrt{\delta\omega}}, \quad (\text{A4})$$

or

$$G^1(0; r_f, r_i) = \frac{4r_i}{r_i + r_f} \int_0^\infty \frac{d\delta\omega}{2\pi} e^{-i\delta r \delta\omega} - \frac{4r_i}{r_i + r_f} \int_\infty^0 \frac{d\delta\omega}{2\pi} e^{i\delta r \delta\omega}, \quad (\text{A5})$$

which leads to (after changing variable  $\delta\omega \rightarrow -\delta\omega$  in the second term of this expression)

$$G^1(0; r_f, r_i) = \frac{4r_i}{r_i + r_f} \int_{-\infty}^\infty \frac{d\delta\omega}{2\pi} e^{-i\delta r \delta\omega} = \frac{4r_i}{r_i + r_f} \delta(\delta r). \quad (\text{A6})$$

Coming back to Eq. (A1) with non zero  $Y$ , we have

$$G^1(Y; r_f, r_i) = \frac{2r_i}{r_i + r_f} \sqrt{\frac{1}{\tilde{\omega} D}} \int_{\tilde{\omega} - i\infty}^{\tilde{\omega} + i\infty} \frac{d\omega}{2\pi i} \frac{e^{\omega Y - \delta r \sqrt{\frac{\omega - \tilde{\omega}}{D \tilde{\omega}}}}}{\sqrt{\omega - \tilde{\omega}}}. \quad (\text{A7})$$

This integral can be evaluated using the method of steepest decent, with the the saddle point in  $\omega$  determined by:

$$Y - \frac{\delta r}{2} \frac{1}{\sqrt{D \tilde{\omega}}} \frac{1}{\sqrt{\omega - \tilde{\omega}}} = 0, \quad (\text{A8})$$

In the limit  $\omega \gg \tilde{\omega}$ , Eq. (A8) leads to the following saddle point value:

$$\omega_{SP} = \left(\frac{\delta r}{2}\right)^2 \frac{1}{Y^2} \frac{1}{\tilde{\omega} D}, \quad (\text{A9})$$

and to the asymptotic behavior of the Green's function:

$$G^1(Y; r_f, r_i) = \sqrt{\frac{1}{2\pi Y \tilde{\omega} D}} e^{-\frac{(\delta r)^2}{4Y \tilde{\omega} D}}, \quad (\text{A10})$$

which is valid for  $\omega_{SP} \gg \tilde{\omega}$ , or  $\omega \sim 1/Y \gg \tilde{\omega}$ , or  $Y \ll \frac{1}{\tilde{\omega}}$ .

Now we consider Eq. (37). Here there are complex conjugates functions and, therefore, the answer is the sum of the real parts of these functions:

$$g(\omega, r_f, r_f) \propto 2 \cos(\pi/6) \int_0^\infty \frac{d\nu}{\sqrt{\nu}} e^{-\xi \nu \cos(\pi/3) - \frac{\nu^3}{3}} \cos\left(\xi \nu \sin\left(\frac{\pi}{3}\right)\right) +$$

$$2 \sin(\pi/6) \int_0^\infty \frac{d\nu}{\sqrt{\nu}} e^{-\xi \nu \cos(\pi/3) - \frac{\nu^3}{3}} \sin(\xi \nu \sin(\frac{\pi}{3})). \quad (\text{A11})$$

Because  $\xi$  and  $\delta\omega$  are small, while  $\nu$  is the order of 1, we can expand our function with respect to  $\xi \nu$ - term. Integrating this expansion over  $\nu$  we obtain the following result for the first two orders of  $\xi$ :

$$g(\omega, r_f, r_i) \propto \frac{\Gamma(\frac{1}{6})}{3^{2/3}} - \xi^2 \frac{\Gamma(\frac{5}{6})}{8 \cdot 3^{4/3}}. \quad (\text{A12})$$

Taking into account expression for  $\xi$ :

$$\xi = \left( \frac{4\omega}{D\omega_L r_H} \right)^{1/3} \frac{r_i + r_f}{\omega} (\omega - \tilde{\omega}),$$

we obtain finally:

$$g(\omega, r_f, r_i) \propto \frac{\Gamma(\frac{1}{6})}{3^{2/3}} - \left( \frac{4\omega}{D\omega_L r_H} \right)^{2/3} \frac{(\frac{r_i + r_f}{2})^2}{8\omega^2} (\delta\omega)^2 \frac{\Gamma(\frac{5}{6})}{3^{4/3}}. \quad (\text{A13})$$

This answer is also valid for the case when  $\delta\omega/\tilde{\omega} \sim 1$  and  $\xi \sim 1$ . In this case, the series of Eq. (A12) will be convergent due to the  $\frac{1}{n!}$  in  $e^{-\xi\nu}$  expansion. Indeed, we see from Eq. (A12), taking  $\xi = 1$ , that

$$\frac{\Gamma(\frac{5}{6})}{\Gamma(\frac{1}{6}) 8 \cdot 3^{2/3}} \propto \frac{1}{80} \ll 1,$$

is small. The following condition for  $\xi$  arises in this case:  $\xi \leq 3$ , and we obtain the simple estimate for the region of  $\omega$  where the series is still convergent and the given solution is still valid:

$$\frac{\omega}{\tilde{\omega}} \leq 3, \quad (\text{A14})$$

where we still have  $\frac{\delta\omega}{\tilde{\omega}} \leq 2$ . Now, if we go back to the Eq. (26), and taking  $\omega = \tilde{\omega}$ , we see, that the correcting term to Eq. (26) is still small,

$$e^{\frac{D\tilde{\omega}}{\omega(\frac{r_f+r_i}{2})^2}} \sim 1 + \frac{1}{96} \ll 1$$

Therefore, in the case  $\delta\omega/\tilde{\omega} \sim 1$  and  $\xi \sim 1$  we obtained overlapping solutions for Green's function, Eq. (26) and Eq. (A12), which match each other. So, we now know the form of our Green's function in the whole region of positive  $\xi$ .

We also find here the  $G(Y; r_f, r_i)$  function. Performing Mellin transform of Eq. (A11) and integrating over  $\delta\omega$  in the first approximation in  $\xi\nu$  we have:

$$G(Y; r_f, r_i) \propto \int_{i\infty}^{-i\infty} \frac{d(\delta\omega)}{2\pi i} e^{\tilde{\omega} Y + Y \delta\omega - \nu \left( \frac{4}{D\omega_L r_H} \right)^{1/3} \frac{r_i + r_f}{2\tilde{\omega}^{2/3}} \cos(\pi/3) \delta\omega} \int_0^\infty \frac{d\nu}{\sqrt{\nu}} e^{-\frac{\nu^3}{3}}, \quad (\text{A15})$$

or

$$G(Y; r_f, r_i) \propto e^{\tilde{\omega} Y} \int_{-\infty}^\infty \frac{d(\delta\omega)}{2\pi} e^{i\delta\omega(Y - \nu \left( \frac{4}{D\omega_L r_H} \right)^{1/3} \frac{r_i + r_f}{2\tilde{\omega}^{2/3}} \cos(\pi/3))} \int_0^\infty \frac{d\nu}{\sqrt{\nu}} e^{-\frac{\nu^3}{3}}, \quad (\text{A16})$$

or

$$G(Y; r_f, r_i) \propto e^{\tilde{\omega} Y} \int_0^\infty \frac{d\nu}{\sqrt{\nu}} \delta(Y - \nu \left( \frac{4}{D\omega_L r_H} \right)^{1/3} \frac{r_i + r_f}{2\tilde{\omega}^{2/3}} \cos(\pi/3)) e^{-\frac{\nu^3}{3}}. \quad (\text{A17})$$

The final answer, obtained for this Green's function in this asymptotic limit, is:

$$G(Y; r_f, r_i) = \sqrt{\frac{3r_i}{8\pi Y \omega_L r_H D}} e^{\tilde{\omega} Y - \frac{2}{9\sqrt{3}} \frac{D(\tilde{\omega} Y)^3}{(r_f + r_i)^{2/4}}}. \quad (\text{A18})$$



## APPENDIX B

The Eq. (44) has the following form :

$$G^{S-H}(r_f, r_i) = D(\omega; r_f, r_i) + \int \int D(\omega; r_f, r_a) (K^S(r_a, r_b) + K^H(r_a, r_b)) G^{S-H}(r_b, r_i) d^2 r_a d^2 r_b. \quad (B1)$$

We are searching the solution of Eq. (B1) in the form

$$G^{S-H}(r_f, r_i) = \int G^H(r_f, r_a) f(r_a, r_i) d^2 r_a. \quad (B2)$$

Inserting Eq. (B2) in Eq. (B1) we obtain:

$$\begin{aligned} \int G^H(r_f, r_a) f(r_a, r_i) d r_a &= \frac{\delta^2(r_f - r_i)}{\omega} + \frac{\Delta_S}{\omega} \phi(r_f) \int \int \phi(r_a) G^H(r_a, r_b) f(r_b, r_i) d^2 r_a d^2 r_b + \\ &+ \int \int \int D(\omega; r_f, r_a) K^H(r_a, r_b) G^{S-H}(r_b, r_c) f(r_c, r_i) d^2 r_a d^2 r_b d^2 r_c, \end{aligned} \quad (B3)$$

where we used that  $K^S(r_f, r_i) = \Delta_S \phi(r_f) \phi(r_i)$  and  $D(\omega; r_f, r_i) = \frac{\delta^2(r_f - r_i)}{\omega}$ .  
And because (see Eq. (2))

$$G^H(r_f, r_i) = D(\omega; r_f, r_i) + \int \int D(\omega; r_f, r_a) K^H(r_a, r_b) G^H(r_b, r_i) d^2 r_a d^2 r_b \quad (B4)$$

we have:

$$\begin{aligned} \int G^H(r_f, r_a) f(r_a, r_i) d r_a &= \frac{\delta^2(r_f - r_i)}{\omega} + \frac{\Delta_S}{\omega} \phi(r_f) \int \int \phi(r_a) G^H(r_a, r_b) f(r_b, r_i) d^2 r_a d^2 r_b + \\ &+ \int \left( G^H(r_f, r_a) - \frac{\delta^2(r_f - r_a)}{\omega} \right) f(r_a, r_i) d^2 r_a. \end{aligned} \quad (B5)$$

This equation leads to

$$f(r_f, r_i) = \delta^2(r_f - r_i) + \Delta_S \phi(r_f) \int \int \phi(r_a) G^H(r_a, r_b) f(r_b, r_i) d^2 r_a d^2 r_b. \quad (B6)$$

Multiplying both parts of Eq. (B5) on the integral  $\int G^H(r_f, r_a) \phi(r_a) d^2 r_a$  and integrating over  $r_f$  we obtain:

$$\begin{aligned} \int \int \phi(r_a) G^H(r_a, r_b) f(r_b, r_i) d^2 r_a d^2 r_b &= \int G^H(r_a, r_i) \phi(r_a) d^2 r_a + \\ &+ \Delta_S \int \int \phi(r_a) G^H(r_a, r_b) \phi(r_b) d^2 r_a d^2 r_b \int \int \phi(r_a) G^H(r_a, r_b) f(r_b, r_i) d^2 r_a d^2 r_b. \end{aligned} \quad (B7)$$

Eq. (B7) gives:

$$\int \int \phi(r_a) G^H(r_a, r_b) f(r_b, r_i) d^2 r_a d^2 r_b = \frac{\int G^H(r_a, r_i) \phi(r_a) d^2 r_a}{1 - \Delta_S \int \int \phi(r_a) G^H(r_a, r_b) \phi(r_b) d^2 r_a d^2 r_b}. \quad (B8)$$

Now, putting back Eq. (B8) into Eq. (B6) we obtain:

$$f(r_f, r_i) = \delta^2(r_f - r_i) + \frac{\Delta_S}{\omega} \frac{\phi(r_f) \int G^H(r_a, r_i) \phi(r_a) d^2 r_a}{1 - \Delta_S \int \int \phi(r_a) G^H(r_a, r_b) \phi(r_b) d^2 r_a d^2 r_b}. \quad (B9)$$

And, finally, we obtain for the solution of Eq. (B1)

$$G^{S-H}(r_f, r_i) = G^H(r_f, r_i) + \Delta_S \frac{\int G^H(r_f, r_a) \phi(r_a) d^2 r_a \int G^H(r_a, r_i) \phi(r_a) d^2 r_a}{1 - \Delta_S \int \int \phi(r_a) G^H(r_a, r_b) \phi(r_b) d^2 r_a d^2 r_b}. \quad (B10)$$

## APPENDIX C

We search the poles which are the zeroes of denominator

$$1 - \Delta_S \int dr' \int dr'' \phi(r') G_\omega^H(r', r'') \phi(r'') = 0. \quad (C1)$$

To calculate  $G_\omega^H(r', r'')$  in this equation, we use the result of Eq. (26) and Eq. (38) for different regions of  $\omega$ . For  $\omega \gg \tilde{\omega}$  we can use the following asymptotic expression:

$$G_\omega^1(r', r'') = \frac{r''}{\tilde{r}^{1/2}} \sqrt{\frac{1}{\omega \omega_L r_H D}} e^{-\delta r \sqrt{\frac{\omega - \tilde{\omega}}{D \tilde{\omega}} + \frac{1}{96} \frac{D \tilde{\omega}}{\omega (r' + r'')^2}}}, \quad (C2)$$

while for  $\omega \sim \tilde{\omega}$ ,  $\xi \ll 1$ ,  $\frac{\delta \omega}{\tilde{\omega}} \ll 1$ , as well as for  $\xi \sim 1$ ,  $\frac{\delta \omega}{\tilde{\omega}} \sim 1$  we can use the asymptotic answer for Green's function given by Eq. (38):

$$G_\omega^2(r', r'') = \frac{r''}{4} \sqrt{\frac{1}{\omega \omega_L r_H D}} \left( \frac{4\omega}{\omega_L r_H D} \right)^{1/6} \left( \frac{\Gamma(\frac{1}{6})}{3^{2/3}} - \left( \frac{4\omega}{D \omega_L r_H} \right)^{2/3} \frac{(r' + r'')^2}{8\omega^2} (\delta \omega)^2 \frac{\Gamma(\frac{5}{6})}{3^{4/3}} \right). \quad (C3)$$

Let us now consider Eq. (C1) using Eq. (C2) for  $G_\omega^H(r', r'')$ :

$$1 - \Delta_S \int dr' \int dr'' \phi(r') G_\omega^1(r', r'') \phi(r'') = 0. \quad (C4)$$

Using new variables

$$x = \frac{r' + r''}{2}, \quad y = \frac{r' - r''}{2}, \quad (C5)$$

in Eq. (C4), we obtain:

$$\frac{\Delta_S}{\omega - \tilde{\omega}_S} e^{\frac{1}{96} \frac{D \tilde{\omega}_S}{\omega r_S^2}} \sqrt{\frac{\omega - \tilde{\omega}}{D \tilde{\omega}}} \int_0^\infty dy \int_{-\infty}^\infty dx e^{-y \sqrt{\frac{\omega - \tilde{\omega}}{D \tilde{\omega}}}} e^{-\frac{2\Lambda^2}{q_S^2} \cosh(y) e^x}. \quad (C6)$$

Due to the properties of the  $\phi$  functions, the main contribution in the integral comes from the region where  $r \propto r_s$  and, therefore, in Eq. (C6) we have used  $\frac{r' + r''}{2} \approx r_s$  and we defined there  $\tilde{\omega}_S = \frac{\omega_L r_H}{r_S}$ . In the limit of small  $\tilde{\omega} \rightarrow 0$  we have  $y \propto \tilde{\omega}^{1/2} \rightarrow 0$  and, therefore, we can write the integral in the form:

$$\frac{\Delta_S}{\delta \omega} e^{\frac{1}{96} \frac{D \tilde{\omega}_S}{\omega r_S^2}} \sqrt{\frac{\omega}{D \tilde{\omega}}} \int_0^\infty dy e^{-y \sqrt{\frac{\omega}{D \tilde{\omega}}}} \int_{-\infty}^\infty dx e^{-\frac{2\Lambda^2}{q_S^2} e^x}, \quad (C7)$$

or

$$\frac{\Delta_S}{\delta \omega} e^{\frac{1}{96} \frac{D \tilde{\omega}_S}{\omega r_S^2}} \int_0^\infty dy e^{-y} \int dx \phi(x)^2 = \frac{\Delta_S}{\delta \omega} e^{\frac{1}{96} \frac{D \tilde{\omega}_S}{\omega r_S^2}}. \quad (C8)$$

The equation for the intercept of the resulting pole is :

$$1 - \frac{\Delta_S}{\omega - \tilde{\omega}_S} e^{\frac{1}{96} \frac{D \tilde{\omega}_S}{\omega r_S^2}} = 0, \quad (C9)$$

or

$$1 - \frac{\Delta_S}{\omega - \tilde{\omega}_S} \left( 1 + \frac{D \tilde{\omega}_S}{96 \omega r_S^2} \right) = 0. \quad (C10)$$

This leads to the solution:

$$\omega = \Delta_{S-H} = \Delta_S + \tilde{\omega}_S + \frac{D \tilde{\omega}_S \Delta_S}{96 r_S^2 (\tilde{\omega}_S + \Delta_S)}. \quad (C11)$$

In another region of  $\omega$  we assume that the position of the resulting pole  $\omega = \Delta_{S-H}$  may be close to  $\tilde{\omega}_S$ ,  $\Delta_{S-H} = \tilde{\omega}_S + \delta\omega$ , where for  $\delta\omega$  there are two asymptotic limits. The first is the small  $\delta\omega$ ,  $\frac{\delta\omega}{\tilde{\omega}_S} \ll 1$ , and the second for the  $\delta\omega$  of the order of  $\tilde{\omega}_S$ ,  $\frac{\delta\omega}{\tilde{\omega}_S} \sim 1$ . We solve Eq. (49) by using the Green function given by Eq. (C3). Due to the form of functions  $\phi(r)$  the main contribution in integral of Eq. (45) comes from these  $r' \approx r'' \approx r_s$ . Therefore, we perform the integration in Eq. (45) only over the  $\phi(r)$  functions, neglecting the term proportional to  $\delta r$  in the integrand. Using the properties of  $\phi$  function, we obtain

$$\int dr' \int dr'' \phi(r') \phi(r'') \approx 4. \quad (C12)$$

This follows from the fact that

$$\int dr \phi(r)^2 = A \int \frac{dq^2}{q_S^2} e^{-q^2/q_S^2} = 1.$$

When  $\delta\omega$  may be small or of the order  $\tilde{\omega}_S$ , ( $\omega = \tilde{\omega}_S + \delta\omega$ ), i.e.  $\frac{\delta\omega}{\tilde{\omega}_S} \ll 1$  or  $\frac{\delta\omega}{\tilde{\omega}_S} \sim 1$ , we obtain the following equation for resulting pole:

$$1 - \Delta_S r_S \sqrt{\frac{1}{\omega \omega_L r_H D}} \left( \frac{4\omega}{\omega_L r_H D} \right)^{1/6} \left( \frac{\Gamma(\frac{1}{6})}{3^{2/3}} - \left( \frac{4\omega}{D \omega_L r_H} \right)^{2/3} \frac{r_S^2}{8 \omega^2} (\delta\omega)^2 \frac{\Gamma(\frac{5}{6})}{3^{4/3}} \right) = 0. \quad (C13)$$

The solution of this equation for the  $\omega = \tilde{\omega}_S + \delta\omega$  with  $\delta\omega \sim \tilde{\omega}_S$ , up to the order  $(\frac{\delta\omega}{\tilde{\omega}_S})^2$ , is :

$$\omega = \Delta_{S-H} = \tilde{\omega}_S + \delta\omega = \frac{2 \Delta_S^3 r_S}{\tilde{\omega}_S^2 D^2} \left( \frac{\Gamma(\frac{1}{6})}{3^{2/3}} \right)^3. \quad (C14)$$

## APPENDIX D

We again consider our variable  $\xi$ :

$$\xi = \left( \frac{4\omega}{D \omega_L r_H} \right)^{\frac{1}{3}} \left\{ \frac{r_f + r_i}{2} - \frac{\omega_L r_H}{\omega} \right\}.$$

At small values of  $\omega$  we have:

$$\xi \approx - \left( \frac{4}{D} \right)^{\frac{1}{3}} \left( \frac{\omega_L r_H}{\omega} \right)^{\frac{2}{3}}. \quad (D1)$$

We should calculate the contribution of the secondary poles to the second term of the Green function of Eq. (71):

$$G_\omega^{DIS}(r_f, r_i) = \frac{\tilde{g}(\omega, r_f, r_i)}{1 - \Delta_S \int dr' \int dr'' \phi(r') G_\omega^H(r', r'') \phi(r'')},$$

We rewrite this equation in the following form:

$$G_\omega^{DIS}(r_f, r_i) \approx \frac{r_i, r_S}{4 \pi \omega \omega_L r_H D} \left( \frac{4\omega}{\omega_L r_H D} \right)^{\frac{1}{3}} \frac{(\tilde{A}i(\xi; \zeta))_{r_i=r_S} (\tilde{A}i(\xi; \zeta))_{r_f=r_S}}{1 - \Delta_S \frac{r_S}{\sqrt{4 \pi r_H D \omega_L \omega}} \left( \frac{4\omega}{D \omega_L r_H} \right)^{\frac{1}{6}} \tilde{A}i(\xi; \zeta=0)} \quad (D2)$$

In the limit of small  $\omega$  we can neglect 1 in the denominator of Eq. (D2):

$$G_{\omega}^{DIS}(r_f, r_i) \approx - \frac{r_i \Delta_S^{-1}}{\sqrt{4\pi\omega\omega_L r_H D}} \left( \frac{4\omega}{\omega_L r_H D} \right)^{\frac{1}{6}} \frac{(\tilde{A}i(\xi; \zeta))_{r_i=r_S} (\tilde{A}i(\xi; \zeta))_{r_f=r_S}}{\tilde{A}i(\xi; \zeta=0)}. \quad (D3)$$

The secondary pole positions are defined by the zeroes of the  $\tilde{A}i(\xi; \zeta=0)$  function in the limit  $\omega \rightarrow 0$ . For  $\xi$  given by the Eq. (D1) we use the method of steepest descent to estimate this function. Calculated saddle points are equal to  $\pm i\sqrt{\xi}$ . They lead to contribution:

$$\tilde{A}i(\xi; \zeta=0)_{\omega \rightarrow 0} \approx \sqrt{\frac{\pi}{|\xi|}} \sin\left(\frac{2}{3}|\xi|^{3/2}\right), \quad (D4)$$

which together with Eq. (D3) gives:

$$G_{\omega}^{DIS}(r_f, r_i) \approx - \frac{r_i \Delta_S^{-1} \pi^{-1/2}}{(4\omega_L r_H D^2 \omega^2)^{1/3}} \frac{(\tilde{A}i(\xi; \zeta))_{r_i=r_S} (\tilde{A}i(\xi; \zeta))_{r_f=r_S}}{\sin(\frac{2}{3}|\xi|^{3/2})}. \quad (D5)$$

We obtain for the secondary pole positions the following equation ( see also [13], [25]) :

$$\sin\left(\frac{2}{3} \left(\frac{4}{D}\right)^{\frac{1}{2}} \frac{\omega_L r_H}{\omega}\right) = 0, \quad (D6)$$

which leads to

$$\omega_n = \frac{2}{3} \left(\frac{4}{D}\right)^{\frac{1}{2}} \frac{\omega_L r_H}{\pi n}. \quad (D7)$$

Expanding  $\sin$  in Eq. (D5) in the vicinity of  $\omega = \omega_n$  for each  $n$ , we obtain:

$$G_{\omega_n}^{DIS}(r_f, r_i) \approx \frac{r_i 2^{-1/3}}{\Delta_S \sqrt{\pi} D^{5/6}} \frac{(\tilde{A}i(\xi; \zeta))_{r_i=r_S} (\tilde{A}i(\xi; \zeta))_{r_f=r_S}}{(\pi n)^{4/3} (\omega - \omega_n)}. \quad (D8)$$

Integrating over  $\omega$  and closing the contour in  $\omega$  over the positions of the secondary poles we obtain the answer for the contribution of a separate secondary pole:

$$G_n^{DIS}(Y; r_f, r_i) \approx \frac{r_i 2^{-1/3}}{\Delta_S \sqrt{\pi} D^{5/6}} \frac{(-1)^n ((\tilde{A}i(\xi; \zeta))_{r_i=r_S} (\tilde{A}i(\xi; \zeta))_{r_f=r_S})_{\omega=\omega_n}}{(\pi n)^{4/3}} e^{\frac{2}{3} \left(\frac{4}{D}\right)^{\frac{1}{2}} \frac{r_H \omega_L}{\pi n} \ln \frac{s}{q_i q_f}}. \quad (D9)$$

The total contribution of the secondary poles is the sum over all " $n$ ":

$$G^{DIS}(Y; r_f, r_i) = \frac{r_i 2^{-1/3}}{\Delta_S \sqrt{\pi} D^{5/6}} \sum_n (-1)^n \frac{((\tilde{A}i(\xi; \zeta))_{r_i=r_S} (\tilde{A}i(\xi; \zeta))_{r_f=r_S})_{\omega=\omega_n}}{(\pi n)^{4/3}} e^{\frac{2}{3} \left(\frac{4}{D}\right)^{\frac{1}{2}} \frac{r_H \omega_L}{\pi n} \ln \frac{s}{q_i q_f}}. \quad (D10)$$

- 
- [1] E.A. Kuraev, L.N. Lipatov and V.S. Fadin, *Sov. Phys. JETP* **45** (1977) 199; Ia.Ia. Balitsky and L.N. Lipatov, *Sov. J. Nucl. Phys.* **28** (1978) 822; L.N. Lipatov, *Sov. Phys. JETP* **63** (1986) 904.
  - [2] A. Donnachie and P.V. Landshoff, *Nucl. Phys.* **B244** (1984) 322; *Nucl. Phys.* **B267** (1986) 690; *Phys. Lett.* **B296** (1992) 227; *Z. Phys.* **C61** (1994) 139.
  - [3] D. Kharzeev and E. Levin, *Nucl. Phys.* **B578** (2000) 351, [hep-ph/9912216](#).
  - [4] D. Kharzeev, Yu. Kovchegov and E. Levin, *Nucl.Phys.* **A690** (2001) 621, [hep-ph/0007182](#).
  - [5] E. V. Shuryak, [hep-ph/0101269](#); Maciek A. Nowak, E. V. Shuryak, and I. Zahed, *Phys.Rev.* **D64** (2001) 034008; [hep-ph/0012232](#) and references therein.
  - [6] A. B. Kaidalov and Yu. A. Simonov, *Phys. Lett.* **B477** (2000) 163;
  - [7] R.A. Janik and R. Peschanski, *Nucl.Phys.* **B586** (2000) 163; **B565** (2000) 193, [hep-th/9907177](#); R.A. Janik, *Phys.Lett.* **B500** (2001) 118, [hep-th/0010069](#); K. Tuchin, *Phys.Lett.* **B497** (2001), [hep-ph/0007311](#).
  - [8] M. Genovese, N.N. Nikolaev and B.G. Zakharov, *JETP* **81** (1995) 625; B. Z. Kopeliovich, I. K. Potashnikova, B. Povh and E. Predazzi, *Phys. Rev. Lett.* **85** (2000) 507.
  - [9] B.C. Brower, S.D. Mathur and Chung-I Tan, *Nucl.Phys.* **B587** (2000) 249, [hep-ph/0003153](#).
  - [10] L. V. Gribov, E. M. Levin, and M. G. Ryskin, *Phys. Rep.* **100**, 1 (1983).
  - [11] A.H. Mueller, J.-W. Qiu, *Nucl. Phys.* **B268**, 427 (1986); L. McLerran and R. Venugopalan, *Phys. Rev.* **D49**, 2233 (1994); **D49**, 3352 (1994); **D50**, 2225 (1994).
  - [12] J.C. Collins and J. Kwiecinski, *Nucl.Phys.* **B316** (1989) 307.
  - [13] E. Levin, *Nucl.Phys.* **B453** (1995) 303; “*ORSAY lectures on low x deep inelastic scattering*” LPTHE, Orsay 91/02.
  - [14] Yu. V. Kovchegov and A. H. Mueller, *Phys. Lett.* **B439** (1998) 428.
  - [15] N. Armesto, J. Bartels and M.A. Braun, *Phys. Lett.* **B442** (1998) 459.
  - [16] E. Levin, *Nucl.Phys.* **B445** (1999) 481, [hep-ph/9806228](#).
  - [17] M. Ciafaloni, D. Colferai and G.P. Salam, *JHEP* **9910** (1999) 017 and **0007** (2000) 054.
  - [18] M. Ciafaloni, M. Taiuti and A. H. Mueller, *Nucl. Phys.* **B616** (2001) 349, [hep-ph/0107009](#).
  - [19] “*Regge Theory of Low -  $p_T$  Hadronic Interaction*”, editor L. Caneschi, North-Holland, 1989.
  - [20] V. S. Fadin and L. N. Lipatov, *Phys. Lett.* **B429** (1998) 127 and references therein.
  - [21] G. Camici and M. Ciafaloni, *Phys. Lett.* **B412** (1997) 396, **B430** (1998) 349.
  - [22] D.A.Ross, *Phys. Lett.* **B431** (1998) 161.
  - [23] G.P.Salam, *JHEP* **9807** (1998) 019.
  - [24] J. Bartels, A. De Roeck, C. Ewerz and H. Lotter, “*The  $\gamma^*\gamma^*$  total cross section and the BFKL Pomeron at 500 GeV  $e^+e^-$  - linear collider*”, [hep-ph/971050](#); S.J. Brodsky, F. Hautmann and D. E. Soper, *Phys. Rev.* **D56** (1997) 6957.
  - [25] L.P.A.Haakman, O.V.Kancheli and J.K.Koch, *Phys. Lett.* **B391** (1997) 157; *Nucl. Phys.* **B518** (1998) 275.
  - [26] C.López and F.J.Ynduráin, *Phys.Rev.Lett.* **44** (1980) 1118; C.López and F.J.Ynduráin, *Nucl.Phys.* **B171** (1980) 231; A. Donnachie and P.V. Landshoff, *Phys. Lett.* **B437** (1981) 408; R.K.Ellis, Z.Kcenszt and E.Levin *Nucl. Phys.* **B420** (1991) 517.
  - [27] M. Ciafaloni, D. Colferai, G. P. Salam and A. M. Stasto, *Phys. Lett.* **B541** (2002) 314, [hep-ph/0204287](#).
  - [28] E. Levin and C. I. Tan, “*Heterotic pomeron: A Unified treatment of high-energy hadronic collisions in QCD*”, [hep-ph/9302308](#).
  - [29] A. K. Likhoded, N. V. Mokhov and O. P. Yushchenko, “*Bare Pomeron In Inclusive Processes*”, FERMILAB-FN-0504, Jan. 1989; P. V. Chliapnikov, A. K. Likhoded and V. A. Uvarov, *Phys. Lett.* **B215** (1988) 417; A. B. Kaidalov and K. A. Ter-Martirosian, *Sov. J. Nucl. Phys.* **39** (1984) 979 A. B. Kaidalov, *Phys. Lett.* **B116** (1982) 459.
  - [30] D. E. Kharzeev, Y. V. Kovchegov and E. Levin, *Nucl. Phys.* **A699** (2002) 745, [hep-ph/0106248](#).